Performance Assessment of Composite Skirted Ground Reinforcement System in Liquefiable Ground Under Repeated Dynamic Loading Conditions

Vijay Kumar S P (spvijay120596@gmail.com)
Indian Institute of Technology (Indian School of Mines), IIT(ISM) Dhanbad https://orcid.org/0000-0001-5594-7961

Ganesh Kumar Shanmugam
CSIR-CBRI : Central Building Research Institute CSIR, Roorkee

Saurabh Dutta Gupta
Indian Institute of Technology (Indian School of Mines), IIT(ISM) Dhanbad

Research Article

Keywords: Isolation Barrier, Infill material, skirted barrier, Ground motions, repeated un-drained loading

Posted Date: July 7th, 2021

DOI: https://doi.org/10.21203/rs.3.rs-186606/v1

PERFORMANCE ASSESSMENT OF COMPOSITE SKIRTED GROUND REINFORCEMENT SYSTEM IN LIQUEFIABLE GROUND UNDER REPEATED DYNAMIC LOADING CONDITIONS

Vijay Kumar S P

Master of Technology, Earthquake Science and Engineering

Department of Applied Geophysics

Indian Institute of Technology (Indian School of Mines), Dhanbad

Dhanbad, Jharkhand - 826004, India

Email: spvijay.18mt0390@agp.iitism.ac.in

Dr. Ganesh Kumar Shanmugam

Scientist and Assistant Professor

Geotechnical Engineering Division

CSIR – Central Building Research Institute

Academy of Scientific and Innovative Research (AcSIR)

Roorkee, Uttarakhand - 247667, India

Email: ganeshkumar@cbri.res.in

Prof. Saurabh Dutta Gupta

Assistant Professor

Department of Applied Geophysics

Indian Institute of Technology (Indian School of Mines) Dhanbad

Dhanbad, Jharkhand - 826004, India

Email: saurabh@iitism.ac.in

Abstract. Occurrence of earthquake generates both horizontal and vertical ground motions. In saturated sands, combination of generated ground motions and pore water pressures induces soil liquefaction. In this study, a composite skirted ground reinforcement system was developed to mitigate generation of pore water pressure in liquefiable soils and also to attenuate incoming ground motions to the foundation. The composite system contains Poly Urethane foam as an isolation barrier for ground motion attenuation with stone columns for improving both soil densification and drainage. The performance of this composite reinforcement system was evaluated under repeated acceleration loading conditions to estimate its efficiency. For testing, saturated ground model having 40% and 60% relative density was prepared and investigated with and without the composite reinforcement system. Test results showed that, the developed skirted ground reinforcement system effectively mitigates the interaction of incoming ground motions with the foundation and also improves the re-liquefaction resistance of soil compared to that of unreinforced ground.

Keywords: Isolation Barrier, Infill material, skirted barrier, Ground motions, repeated un-drained loading

1 Introduction

Earthquake induced ground motions always pose threats to the safety of infra-structures. When such structures are located in saturated sandy deposits, the failures were mainly due to (i) interaction between the foundation structure and the developed ground motions and (ii) generation of excess pore water pressures which reduces shear strength of saturated soil deposit. To attenuate ground motions developed during dynamic loading, conventional isolation systems were used which minimize incoming horizontal acceleration to the structure. However, only limited studies were available for evaluating the response of isolation system in liquefiable soils. Also, the observed recent repeated earthquake events (i.e. occurrence of continuous foreshock and main shock events etc.) with reported liquefaction and reliquefaction occurrence in sandy deposits recommends evaluating the performance of any ground improvement system under repeated dynamic loading events to estimate its longer performance characteristics.

Generally, generation of excess pore pressure during dynamic loading in saturated sandy deposits reduces shear strength of soil resulting in soil liquefaction. The liquefied ground no longer can support the weight of the overlying structures which leads to the failure of structure. Similarly, during dynamic loading; the structure located near epicenter experiences a combined horizontal and vertical ground acceleration responses which create vertical deformation and failure of structure (Papazoglou and Elnashai 1996). The response of vertical component of ground motion found to be higher in near fault regions, higher magnitude seismic events and in shorter period events relative to the horizontal component (Bozorgnia and CampBell 2003). There are also limited energy dissipation mechanisms available for estimating and minimizing the vertical response of ground motions (Kunnath et al. 2008).

To isolate the structure from ground motion interaction during dynamic loading, different studies have been attempted by various researchers. Majority of the approach adopt development of barrier system to attenuate the incoming ground motions. Woods (1968) performed series of field experiments with open trenches as a barrier for near field and far field isolation. Open or infill trenches were used as vibration barriers and the in-filled trenches with softer materials found to offer better isolation performances (Woods 1968; Dasgupta 1989; Ahmad et al. 1991; Adam et al. 2005). Open and infill trenches were found more effective in damping vertical than horizontal vibrations (Dasgupta 1989; Al-Hussaini and Ahmad 1991; Yang Hung 1997). The isolation performance of open trenches depends on both depth and width. Further, the efficiency reduces when it is located near the source or site (Yang et al. 2018). Soft and low acoustic impedance materials when used as an infill material for trenches found to be an effective vibration isolation barrier option due to its higher damping characteristics (Zeng et al. 2001; Wang et al. 2009; Pu, X., et al. 2018). Foam infill trenches found to be a good vibration isolation barrier for mitigating the vertical vibrations in both active and passive isolation cases (Wang et al. 2006; Majumder and Ghosh 2016; Pu, X., et al. 2018). The deeper the trench, the better is the isolation effect and also the influence of the width comparatively reduces in determining the performance of infill barrier system (Yang, Y.B., and Hung, H.H. 1997; Alzawi and El Naggar 2011; Connolly et al. 2013; Feng et al. 2020; Pu, X., et al. 2018). The efficiency of intermittent foam trenches increases with the increase in frequency of vibrating source and stiffness of sub-soil deposit (Majumder and Ghosh 2016). Overall, the use of PU foam as infill trenches found to be very effective in damping out ground-borne vibrations (Bose, T. and Choudhury, D. 2018). Though detailed studies on ground motion mitigation using PU foam

barrier system were available, studies relating to its performance assessment in mitigation of ground motions in saturated sandy deposit were limited. Considering the liquefaction susceptibility in loose saturated sands, a good barrier accompanied with draining characteristics is required for improving the seismic response of such ground deposits. Hence, there is a need for developing a composite effective energy dissipation system which can attenuate ground motions interaction with the structure and also to improve the seismic resistance against liquefaction in liquefiable deposits.

In this study, an attempt has been made to develop a synergized isolation barrier system in the form of definite boundary of infill material that can absorb the incoming ground motions generated during dynamic loading and also contain suitable reinforcement member which can reinforce and minimizes generation of pore water pressures during dynamic loading. For developing isolation barrier system, commercially available PU foam material was selected as an infill material. Since, the barrier was installed within liquefiable soil ground; geotextile material was encased around the PU foam barrier to minimize clogging and to prevent soil-foam intrusion. For improving reinforcement and drainage characteristics, the barrier system was installed together with stone column improvement system within the confined zone of saturated ground. This combined reinforcement technique otherwise called as composite skirted ground reinforcement system provides an effective solution in mitigating ground motion interaction with the sub-structure and also resists generation of pore water pressures inside the saturated ground during dynamic loading. The performance and efficiency of the developed skirted ground reinforcement system was evaluated under repeated incremental acceleration loading conditions. The selection of repeated loading events was done similar to observed continuous foreshock and aftershock events experienced during an earthquake incidence. For experimental studies, saturated sand deposit having 40% and 60% density was prepared and tested with and without the composite barrier reinforcement system. The model ground was subjected to repeated sinusoidal loading of 0.1g, 0.2g, 0.3g and 0.4g acceleration intensities with 5 Hz frequency. The provided repeated sequential acceleration intensities tend to simulate the repetition of medium to severe earthquake motion conditions pertaining to the ground model. A constant excitation frequency of 5 Hz was maintained for all the tests in order to produce medium to high seismic conditions in the ground (Murali Krishna, A., & Madhavi Latha, G. 2007; Singh, H.P., 2009). The acceleration loadings were applied subsequently to the ground only after complete dissipation of generated pore water pressures from previous loading. The generation of pore water pressures, pore pressure ratio, acceleration response, foundation settlement and soil displacement with and without provision of skirted ground reinforcement system were studied and presented. From experimental tests performed, it can be observed that installation of composite skirted isolation barrier system effectively mitigates ground acceleration and also mitigates generation of pore water pressures during repeated loading. With the proposed skirted ground reinforcement, about 80% average reduction in generated peak ground acceleration was recorded near the footing model and the average foundation settlement of embedded footing model found to reduce by about 75%. Similarly the system reduces generation of pore water pressure to about 50% in 40% density condition and about 60% in 60% density condition. Even at repeated loading, the confined skirted ground reinforcement system showed better performance than untreated ground.

2 Soil Ground Model

For experimental studies, soil sample collected from solani river bed in Roorkee, Uttarakhand was used. The soil was classified as poorly graded sand (SP) as per Indian standard classification [IS 2720 Part 4 – 1985]. Fig.1 shows the grain size distribution curve for the obtained soil. It can be seen that, the soil falls within the range of potentially liquefiable sand proposed by (Tsuchida, H. 1970; Xenaki and Athanasopoulos 2003) indicating that the soil is more susceptible to liquefaction. The other index properties of the sand are listed in Table 1.

2.1 PU Foam material properties

Polyurethane foam (PUF) material which is well known for high resilience, abrasion and vibration absorption characteristics in its cured state was selected for developing isolation barrier in the model ground. PU foams have been generally used in shaking table experiments as an absorbing boundary member. The beneficial absorbing and damping characteristics of PU foam motivated to use them as an isolation barrier inside the liquefiable deposit to evaluate its dynamic performance under repeated shaking events. The PU foam was procured in liquid form which had two components, resin and hardener both of density 11 kN/m^3. Procured PUF had a capacity of expanding up to 30 times its original volume. Considering the mixing and application losses involved, a nominal volume expansion factor of 25 times was fixed. For developing barrier model, the liquid PU foam was poured inside the prepared mold and barrier models were prepared. The properties of PU foam material are given in Table 2.

2.2 Geotextile

A 1.5 mm thick non-woven needle punched polypropylene geotextile has been used for encasing the PU foam barrier system. The tensile strength, mass per unit area, opening size and permeability are 14 kN/m, 0.2 kg/m^2, 0.085 mm and 0.0036 m/s respectively. The provision of geotextile around the barrier prevents the migration of finer soil particles inside the barrier.

2.3 Stone Aggregates

Uniformly graded angular granite chips of size range 2 mm to 10 mm have been used for constructing stone columns inside the model ground. The stone aggregates used in all the tests were compacted to a dry density of 16 ± 0.2 kN/m^3 corresponding to a relative density of 73% (representing field situation). The peak angle of frictional resistance of stone aggregates obtained using the large direct shear box tests is 42º.

3 Preparation of PUF isolation barrier

The quantity of foam liquid required for the developing the barrier system was estimated and prepared by mixing the resin and hardener in a ratio of 1:1.The generation of pore water pressures from bottom to top during dynamic loading resulted in uplifting of the plane foam barriers prepared during initial studies. To mitigate uplift and to create effective anchorage characteristics, the barrier was modified with inverted 'T' shape section. For experimental testing two inverted T-shaped model having dimensions of Heel: 500 mm × 200 mm × 50 mm, Toe: 500 mm × 100 mm × 50 mm and Stem: 500 mm × 50 mm × 350 mm was prepared and placed inside the prepared ground perpendicular to shaking direction at 650 mm c/c spacing between the stems to confine the installed scaled down foundation model. The dimensions of PUF barrier model was fixed by considering a scale-down factor of 1:20 with respect to its in-situ installation. Initially, the molds were prepared according to the required dimensions and then the prepared foam liquid was poured in to the mold for barrier development. A sufficient hardening time of about 20 - 30 minutes was allowed to achieve the definite barrier shape. Since the ingress of finer silt particles to the barrier model can create clogging; geotextile material was wrapped around the surface of foam barrier. Fig.2 (a) and Fig.2 (b) shows, the construction and casting details of PU foam barrier. Schematic view of constructed foam barrier with dimensions is shown in Fig 2 (c).

4 Experimental setup and sample preparation

The experimental setup consists of the uniaxial shaking table having dimensions of 2.0 m × 2.0 m of steel table mounted on rails. The load-carrying capacity of the table is 30 kN. The table is attached to a servo-hydraulic actuator, which facilitates the movement of the table. The maximum stroke length of the actuator is $\pm$160 mm. The table works with an operating frequency range of 0.01 to 50 Hz with a maximum peak velocity of 2 m/s and acceleration range from 0.001g to 1g. The entire operation of the shaking table was performed through a digital controlled data acquisition system. The control unit is capable of accepting sine, rectangular, triangular, and reduced scale earthquake motions as input motions.

The laboratory model tests were performed inside a rigid Perspex rectangular tank having dimensions 1.4 m × 1.0 m × 1.0 m. Since the rigidity of the container could generate boundary effects in the soil sample (Whitman and Lambe 1986; Lee et al. 2012); a 50mm thick expanded poly-ethylene (EPE) foam was placed near the boundary of the tank at right angles to the shaking direction to minimize boundary effects (Bhattacharya et al. 2012; Lombardi and Bhattacharya 2012; Lombardi et al. 2015; Punetha 2016; Padmanabhan, G and Shanmugam, G.K. 2020). Before experimental testing, the bottom of the test tank was made rough by sand blasting to ensure the transfer of shear stress and input motions from the base of the tank to the prepared ground.

Vaid and Negussey 1988, through experimental results concluded that; maximum homogeneity in sample preparation can be achieved using wet sedimentation technique. Hence, wet sedimentation technique was selected for sample preparation in this study. For testing, a 600 mm thick saturated sand bed having 40% and 60% relative density was prepared inside a thick perspex glass tank. The weight of sand and quantity of water required to occupy

the desired volume corresponding to the relative density (i.e. 40% and 60%) inside the tank was calculated based on the following procedure (Muley, P., et al. 2012).

Preparation of Samples

The following steps were adopted for the preparation of a saturated sand deposit for the experimental studies

I. The void ratio (e) corresponding to a relative density (D_r) of the sand was calculated as

$$e = e_{\max} - D_R\left(e_{\max} - e_{\min}\right) \quad (1)$$

Where e_{max} is the maximum void ratio, e_{min} is the minimum void ratio and e is the desired void ratio for the proposed relative density (D_r).

II. Knowing the value of the desired void ratio from the above equation, the dry unit weight of the sand is determined from the equation

$$\gamma_d = \frac{G}{1+e}\gamma_w \quad (2)$$

Where γ_w is the unit weight of the water (taken as 10 kN/m^3), γ_d is the dry unit weight of the sand (kN/m^3) and G is the specific gravity.

III. Assuming the height of the tank to be filled with soil sample i.e. 600 mm, the volume (V) occupied by the sample in the tank was determined using the plan dimensions of the tank, that is 1300 mm × 1000 mm after deducting foam thickness on both sides of the tank.

IV. The dry weight of the sand required to fill the tank to achieve the desired relative density and height was determined from the following equation

$$W_d = \gamma_d \times V \quad (3)$$

V. The water content required to achieve full saturation of sand sample was calculated from the following equation.

$$eS = wG \quad (4)$$

Where, S is the saturation level of the sand sample (for fully saturated sample S = 1).

VI. From the required amount of water content, the weight of water required for the sample preparation is calculated from the following equation

$$W_w = w \times W_d \quad (5)$$

VII. The quantity of water required for preparing 40% and 60% density ground with full saturation was calculated using the above relationship.

The estimated total quantity of sand and water was divided into three layers and the ground bed was formed through layer by layer to achieve more uniformity in sample preparation. Initially, the tank was filled with calculated quantity of water to the pre-calculated depth for the first layer. Then, sand was rained down in to the container at calculated height through a conical hopper arrangement having an inverted solid cone with a 60° angle attached at the end. The method of sand pouring through a conical hopper arrangement was selected for achieving uniformity in

sample preparation (Varghese and Latha 2014). The height at which the sand has to be poured for achieving respective density was pre-calculated by performing repeated relative density tests as per IS 2720 – Part XIV and ASTM D4254 – 2006. From the height of fall experiments, the height of pouring has been decided to be 110 mm and 160 mm for achieving 40% and 60% relative densities respectively. The sample preparation procedure was repeated up to the total depth of 600 mm. All the experiments were conducted on saturated ground having 40% and 60% density. The schematic diagram of the shaking table test setup and method of sample preparation is shown in Fig. 3 (a - d). Thus, the untreated soil ground prepared was left undisturbed for 24 hours for achieving uniform saturation.

4.1 Methodology adopted for the treated ground

4.1.1 Installation of PU foam barrier system in to the prepared ground

The procedure adopted for PU foam barrier installation is explained in this section. The developed inverted "T" shaped PU foam barrier model was placed on the prepared saturated ground after completion of initial 300 mm depth. After placing the barrier over 300 mm thick deposit, sample preparation was continued up to selected 600 mm height. Thus, the prepared PU foam barrier was buried inside the ground deposit with 50 mm portion of stem projecting above the model ground. For estimating ground acceleration response below the base of the barrier system and below the foundation model, three accelerometers A1, A2 and A3 were placed inside the soil bed. The accelerometers A1 and A2 were placed within the confined area at 400 mm and at 100 mm depth and A3 being outside the barrier area at 100 mm depth from top ground surface respectively. Stone column installation was then carried out within the confined portion i.e. within the confined space of 400mm between the PUF barriers i.e. excluding base slab dimension of the installed barrier model.

4.1.2 Installation of Stone columns

Generally, effect of soil densification and drainage effects due to stone columns installation improves the seismic response of liquefiable ground. Hence, the stone columns were selected in this study and installed together within the isolated barrier system. The stone columns were installed after completion of ground preparation with PU foam barrier system. For experimental testing, 4 stone columns having diameter 110 mm with 275 mm c/c spacing and having an area replacement ratio 2.5% was installed up to 600 mm depth. All the stone columns were installed using displacement method [IS 15284 (Part1): 2003] for achieving soil densification in the ground. A casing pipe having outer diameter equivalent to stone column diameter was selected and driven in to the prepared ground through vibration. The soil inside the casing was removed using an auger. Then, the stone aggregates were placed in 4 layers of 150 mm depth. After filling each layer, the stones were compacted and the casing was lifted to a height of 100 mm for achieving continuity in column preparation. The procedure was repeated up to the height of 600 mm. The procedure of stone column installation by displacement method is shown in Fig. 4 (a-c).

For monitoring pore pressure generation during shaking, two glass tube piezometers were connected to the pore pressure cells placed at the center of the tank at 400mm and 200mm depth from the prepared ground bed surface respectively. Fig. 5(a) and Fig. 5(b) show the finished plan and sectional view of the test set-up and instrumentation details for monitoring pore pressure generation and acceleration response during testing. The detailed experimental schedule adopted for assessing the performance of barrier system in liquefiable soils is shown in Table 3.

4.2 Estimation of foundation settlement

To study the foundation response with and without barrier system under repeated acceleration events, a scaled down shallow footing model was used in this study. After the installation of stone columns and PU foam barrier system, the foundation model was placed at center inside the confined area at 35 mm depth for estimating foundation settlement during testing. The procedure adopted for scaling of the foundation model is based on dynamic similitude laws given by (Moncarz and Krawinkler 1981) is shown in Eq. 6

$$N_{(EI)} = N_{(K)} \times N_{(L)}{}^{3} \tag{6}$$

Where,

$N_{(EI)}$ = Scale factor for flexural rigidity

$N_{(K)}$ = Scale factor for stiffness

$N_{(L)}$ = Scale factor for linear dimensions

A scale down factor (n) of 10 was used to model shallow footing. The foundation was modeled with 115 mm length, 115 mm wide and 30 mm thick using a steel material having modulus of elasticity 200GPa. Using displacement transducers, foundation displacement under dynamic loading was monitored.

4.3 Density evaluation

The density of the prepared ground was investigated using a digital static cone penetrometer (DCPT). The digital cone penetrometer consists of a drive cone assembly having a 60° cone angle and an area of 150 mm^2, extension rods and a digital display unit attached load cell. The cone penetrometer assembly was pushed vertically into the prepared ground at the rate of 10 mm/sec [IS 4968 (Part III) – 1976 and ASTM D3441 – 16] and corresponding penetration resistance values at every 100 mm penetration were recorded. The relative density of the sand deposit at different depths was estimated using Eq. 7 proposed by Jamiolkowski et al. 2003.

$$D_R = 100\left[0.268 \times \ln\left(\frac{q_t/\sigma_{atm}}{\sqrt{\sigma'_{vo}/\sigma_{atm}}}\right) - 0.675\right] \tag{7}$$

Where, D_R is the relative density of the sample as a fraction, q_t is the cone penetration resistance in kg/cm^3 and σ'_{vo} is the effective overburden pressure in kg/cm^2 .

The cone penetration tests were conducted continuously before and after application of repeated acceleration loading to assess the improvement in density for the treated and untreated ground.

4.4 Selection of repeated incremental acceleration loading conditions

The objective of the study is to develop composite barrier to effectively absorb ground motions and to mitigate pore water pressure generation in liquefiable deposits during dynamic loading. To assess this composite barrier performance, the experiments were performed with repeated acceleration loading conditions. The selection of repeated loading was based on the observed continuous earthquake events and associated foreshock and aftershock movements experienced during Christchurch earthquake 2010-11, Japan earthquake 2011, Nepal earthquake 2015, Kumamoto earthquake 2016, and Indonesia earthquake 2018. The case studies showed the occurrence of liquefaction and reliquefaction in saturated ground and resulting failure of infra-structures. Considering the above cases, the developed composite barrier system was tested under repeated incremental acceleration loading conditions to evaluate the behavior of treated and untreated liquefiable deposits. For experimental testing, sinusoidal wave having acceleration 0.1g, 0.2g, 0.3g and 0.4g at 5 Hz constant frequency was selected and applied to the prepared ground. The time history for the selected input motions is shown in Fig. 6 (a to d). The selected acceleration loadings (0.1g, 0.2g, 0.3g and 0.4g at 5 Hz frequency) represents medium to severe earthquake motions in real field conditions (Robertson and Campanella 1985).

The continuous incremental acceleration loading was applied to the ground bed only after the complete dissipation of generated excess pore water pressure from previous acceleration loading. Using glass tube piezometers, the generation and dissipation of pore water pressure was monitored. After complete dissipation, subsequent incremental loading was applied. The procedure was repeated up to 0.4g acceleration loading.

5 Results and Discussions

5.1 Acceleration Response for the untreated and treated ground

The performance of composite barrier system in isolating ground motions was evaluated using accelerometers. Three accelerometers A1, A2 and A3 located at 0.4m, 0.3m and 0.1m depth respectively was used for the study in case of untreated ground. In composite barrier reinforced ground, accelerometers A1 and A2 were placed within the confined zone at 0.4m and 0.1m depth respectively and one accelerometer A3 outside the composite barrier system at 0.1m depth respectively to compare the acceleration response of treated and untreated ground during shaking. Typical acceleration response for the untreated and treated ground (i.e. within the confined zone) at 0.2g acceleration loading for 40% density ground and at 0.3g acceleration loading for 60% density ground is shown in Fig. 7 (a) and 7 (b) respectively. The obtained test results after 0.1g shaking in 40% density treated ground and test results up to 0.2g shaking in 60% density treated ground showed very negligible response as compared to untreated ground. Hence only test results comparing untreated and treated conditions for 0.2g shaking incase of 40% density ground and for 0.3g shaking in case of 60% density ground is shown. The acceleration response of unreinforced model ground is indicated by green colour and that of skirted barrier reinforced model ground is indicated by blue colour in Fig. 7 (a) and 7 (b). It can be seen that, provision of isolation barrier attenuate the incoming motions inside the confined zone. About 72% reduction in acceleration response at 0.2g shaking in case of 40% density ground and about 76% reduction at 0.3g shaking in case of 60% density ground was observed with the provision of skirted barrier reinforcement system. Due to contact instability between accelerometer and soil bed more disturbances were observed in the accelerometers during repeated loading. The disturbance increases after 0.2g acceleration loading in case of 40% ground and after 0.3g acceleration loading in case of 60% density ground due to which the response patterns were highly inconsistent. Hence, only the obtained acceleration response at 0.2g loading for 40% density ground and acceleration response at 0.3g loading for 60% density ground with and without barrier system are compared in Fig. 7. However, data for all the acceleration loading for both 40% and 60% ground conditions was converted into frequency domain and compared. The obtained peak spectral amplitude for the skirted and untreated ground under repeated loading is shown in Fig. 8 (a) and 8 (b). Similar to acceleration response as discussed, the maximum spectral acceleration amplitude also reduces with the provision of skirted barrier system. The reduction observed in spectral amplitude was about 75% to 77% for 40% density ground and 57% to 61% for 60% density ground under repeated incremental loading conditions. Comparatively, barrier system was found more effective in 40% density ground than 60% density ground. The reduction in spectral amplitude response clearly validates the performance of composite isolation barrier system in attenuating the incoming motions in to the structure.

The performance of isolation barrier in attenuating the generated ground motions was further verified by comparing the obtained acceleration response between the accelerometer placed outside the barrier confined zone and the accelerometer placed within the confined zone of treated ground at 0.1m depth from ground surface. The comparison of acceleration response is shown in Fig 9 (a) and 9 (b) for 40% density and 60% density treated ground conditions respectively. Similar to untreated and treated ground response, acceleration response inside the confined zone found to be minimum than accelerometer response obtained outside the confined zone. The average damping offered in confined zone was about 90% for 40% ground conditions and 86% for 60% ground conditions. The response is mainly due to the improvement in density and reduction in pore pressure generation offered by the composite barrier system. Within the confined zone; the installed stone column minimizes generation of pore water pressures and the provision of PU foam barrier attenuate the incoming ground motion response.

To evaluate the performance of composite isolation barrier further, an amplitude reduction ratio (ARR) defined as the ratio of maximum spectral amplitude of vibration for the treated ground to that of untreated ground was developed as shown in Fig.10 for 40% and 60% density ground. When the loose ground is subjected to shaking, occurrence of soil densification improves vibration attenuation. In case of 40% ground, ARR for the barrier system showed comparatively higher values during initial loading indicating lower vibration attenuation and the performance of composite barrier system improved during repeated shaking. ARR value increased up to 0.2g acceleration loading indicating the development of dilation effect and soil densification during low to medium intensity shaking conditions. In 60% density ground which had a relatively higher initial densification, the continual reduction in ARR value is observed up to 0.3g shaking which may be due to well established soil dilation effects with associated densification that improved the performance of the barrier system. However under repeated un-drained loading conditions, the efficiency of barrier system slightly reduced at 0.4g shaking. In both 40% and 60% dense ground, with improvement in density, the efficiency of vibration attenuation in the composite barrier system decreases due to development of soil dilation and pore pressure generation. The observations concluded that with skirted ground reinforcement in ground model, the amplitude reduction ratio found better during medium to high intensity shaking events and at low acceleration loading conditions; however the selected composite barrier reinforcement system does not effectively mitigate generation of pore water pressures.

5.2 Generation of pore water pressures for the treated and untreated ground

The generation of pore water pressure during dynamic loading induces reduction in shear strength causing soil liquefaction. The influence of generated pore water pressures and the estimated pore pressure ratio with and without barrier system is explained in this section. The pore water pressure was continuously monitored using two glass tube piezometers placed at 0.2m and 0.4 m depth from prepared ground bed surface. For repeated loading tests, subsequent acceleration loading was applied only after complete dissipation of generated pore water pressures from previous loading i.e. after application of 0.1g acceleration loading, variations in pore water pressure was continuously monitored through piezometers and after complete dissipation of generated pore water pressures, 0.2 g acceleration loading was applied to the ground. The same procedure is repeated up to 0.4g loading. Fig. 11 and 12

shows the obtained pore pressure response for the treated ground and untreated ground under repeated acceleration loading conditions in 40% and 60% RD model grounds respectively. At 40% density treated ground, generation of pore water pressure was found to be lesser than untreated ground which is shown in Fig. 11 (a-d). The total average reduction in pore water pressure was about 40% to 50% for 0.1g to 0.4g acceleration loading as compared to untreated ground. The drainage path created by the stone columns within the confined zone minimizes pore pressure generation and improves deposition of suspended soils during shaking which resulted in improvement in density. Provision of drainage and continuous improvement in soil densification improves the seismic response of the ground during repeated loading. The occurrence of non-uniform soil densification was observed under repeated un-drained loading due to the continuous generation of pore water pressures and non-uniform soil deposition after loading. The non-uniformity in soil deposition due to repeated loading was further verified using cone penetration experiments. In case of treated ground, the provided granular columns within the confined zone delays and dissipates pore water pressure continuously. However, under high intensity shaking conditions, dissipation efficiency slightly reduced which may be due to inadequate area replacement ratio and clogging effects in stone column reinforcement. However in all the loading conditions, the generated pore water pressure found to be less compared to untreated deposits. The occurrence of non-uniform soil densification in the case of untreated ground resulted in rapid generation of pore water pressures from bottom to top during each loading and in the absence of drainage medium; liquefaction and reliquefaction was observed at shallow depth in all the loading conditions due to less overburden pressure. Compared to 40% ground, time for pore pressure generation was found higher in 60% density ground which can be seen from Fig. 12 (a-d). However, generated pore water pressures induce liquefaction and reliquefaction in untreated ground. This suggesting that, in addition to soil densification; provision of drains in liquefiable deposits also plays a major role in improving seismic response against reliquefaction in case of repeated acceleration loading events. At 60% density ground, generation of pore water pressures was not observed in the case of 0.1g acceleration loading which validates the influence of soil densification together with drainage layer. Further, the reduction in pore water pressure was about 80% to 40% for 0.2g to 0.4g acceleration loading for the treated ground. With the installation of stone columns, time for generation of pore water pressure increases and enhances seismic resistance of soil against liquefaction together with lateral confinement system. Thus it can be concluded that, soil densification together with drainage medium improves the seismic response of saturated grounds under repeated acceleration loading events.

The performance of the treated ground was further validated by estimating the pore pressure ratio of the treated and untreated ground.

The pore pressure ratio was estimated using the formula

$$r_u = \frac{U_{excess}}{\sigma'_{vo}} \tag{8}$$

Where, U_{excess} is the excess pore water pressure and σ'_{vo} is effective overburden pressure which can be estimated as follows

$$\sigma'_{vo} = \sigma - u \quad (9)$$

The soil is considered to be liquefied losing its shear resistance when the pore water pressure ratio reaches unity (Seed and Lee 1966). The estimated pore pressure ratio for the treated and untreated ground having 40% and 60% density is shown in Fig 13 and 14 respectively. As mentioned, installation of stone column together with PU foam performs better in mitigating the generation of pore water pressure and improving the seismic resistance at 40% ground conditions compared to untreated ground. However, at 60% density ground, due to the additional improvement in initial density, the stone column and barrier installation further enhanced the performance of the system.

When the unreinforced ground was subjected to acceleration loading, generation of pore water pressures induces reduction in strength causing liquefaction. After shaking, the suspended particles settled down forming a consolidated soil ground. Due to occurrence of soil consolidation, density increases after acceleration loading. However, due to non-uniformity in soil deposition, the improvement in density was not uniform with depth. During repeated loading, the consolidated ground generates pore water pressure and becomes unstable due to absence of drainage characteristics. It was evident that upward drainage occurred from bottom to top made soil at shallow depth more susceptible to re-liquefaction. Thus, the variation of excess pore water pressure ratio estimated from top piezometer (placed at 0.2 m depth) with respect to time for both untreated and treated ground having 40% and 60% relative density soil ground subjected to sequential incremental acceleration is shown in Fig. 13 (a-d) and Fig. 14 (a-c) respectively. With the increase in acceleration loading, time for generation of pore water pressure reduces causing reliquefaction in subsequent loading. Provision of composite barrier system delays and minimizes generation of pore water pressure that improves seismic resistance of the ground which can be seen from Fig. 13 and 14 for 40% and 60% ground. It can be clearly seen that estimated pore pressure ratio in skirted ground reinforcement is found much lower compared to unreinforced condition for the initial 0.1g acceleration loading. This was mainly due to the combined improvement in density and drainage induced by the skirted ground reinforcement system. However, under subsequent loading, the efficiency of skirted ground reinforcement slightly decreases due to continuous generation of pore water pressures and possibility of clogging. The observed average reduction in pore pressure ratio values with reinforcement for both the treated grounds were found to be higher for initial accelerations (i.e., 0.1g and 0.2g is about 45% to 70%) whereas during high and intense acceleration loading, only 41% to 52% reduction in pore pressure generation was observed. This suggests the need for proper area replacement ratio for improving the seismic resistance of the ground. Overall, the installed barrier system performs effectively as compared to untreated ground. The influence of drainage medium during repeated shaking events is further analyzed by comparing time of liquefaction and discussed elaborately in the following section.

5.3 Time Taken for peak pore pressure attainment

The generated pore water pressure inside the 40% and 60% density model ground under repeated incremental sequential incremental acceleration loading showed that the time taken for attainment of peak value of excess pore water pressure decreases with increase in acceleration loading which is shown in figure 15 (a-b) for a shallow depth. This found similar with Ye et al. 2018, suggesting that resistance of sand to re-liquefaction is less than that to first liquefaction despite of the increase in their density. It can also be seen that during subsequent loading, the time taken for liquefaction initiation is delayed when the ground is reinforced with composite barrier system. However, from both Figure 15 (a) and 15 (b) it can be observed that during higher acceleration loading the performance of reinforced ground with 40% and 60% density found slightly reducing. This may be due to possibility of column clogging which affects the drainage characteristics. Additionally, the selected area replacement ratio also contributed in reducing the performance of reinforcement system during higher intensity loading. However, from the observed pore pressure generation time and improvement in soil resistance, the skirted ground reinforcement is found more durable even during repetitive cyclic loading as it not only confines the ground but also delays the time taken for liquefaction occurrence by provision of effective drainage system.

5.4 Variation in Relative Density

The application of repeated acceleration loading induces repetitive soil rearrangement causing variation in soil density for both treated and untreated ground. The variation in relative density after each loading was estimated using digital cone penetration tests. Tests were conducted on untreated and treated ground before and after application of acceleration loading. From the obtained cone penetration resistance, the relative density of the untreated and treated ground was estimated. The obtained cone penetration resistance for the 40% and 60% untreated and treated ground is shown in Fig. 16 (a) and 16 (b). It can be seen from both untreated and treated ground, penetration resistance increases after application of acceleration loading. The improvement in penetration resistance verified soil densification during repetitive loading. The estimated relative density values for the treated and untreated deposits are also shown in Fig.17 (a) and 17 (b). Occurrence of non-uniform soil deposition was evident from Fig.16 (a-b) and 17 (a-b). In untreated ground, the variation in density after each loading was about 4% to 12% for 40% ground and 5% to 9% for 60% ground for the applied acceleration loading 0.1g to 0.4g. The variation in density was not uniform with depth having maximum at bottom and minimum at top. Under un-drained repeated loading, the untreated ground generates pore water pressure from bottom to top. In the absence of drainage, the generated pore water pressures made soil at shallow depth more susceptible to liquefaction and reliquefaction. The same was verified from the estimated pore pressure ratio for the shallow depth.

In case of treated ground reinforced with composite barrier system, provision of stone columns within the confined zone limits generation of pore water pressure and facilitates rapid dissipation thereby improving rate of soil deposition. This results in improvement in soil density under repeated loading. Compared to untreated ground, the improvement in soil density was about 9% to 15% higher for 40% ground and 7% to 10% higher for 60% ground. Through improvement in density, the combined barrier and granular columns improves the resistance against

reliquefaction under repeated acceleration loading. From these observations, it is evident that the prepared ground model with skirted ground reinforcement improves density of the ground through confinement using PUF barriers and with stone columns. Also, this confinement system made the soil at shallow depth more stable and resistant against liquefaction and reliquefaction through soil densification and drainage.

5.5 Change in void ratio

The change in average void ratio (e) of the prepared ground model under repeated incremental sequential sinusoidal loading was calculated using the relative density (D_R) expression

$$e = e_{\max} - D_R \left(e_{\max} - e_{\min} \right) \tag{12}$$

Where, $e_{\max}$, $e_{\min}$ are maximum and minimum void ratio of the sand as given in Table 1 and D_R is the estimated relative density after each loading. Figure 18 (a) and 18 (b) shows the void ratio variation with depth for the untreated and treated ground. It was observed that the void ratio for the treated and untreated ground decreases with the increase in acceleration loading due to occurrence of soil densification. The variation in void ratio under repeated loading was also found similar to that of Ye et al. 2018. Comparatively, the reduction of void ratio in treated ground was found higher than that in untreated ground under 40% and 60% ground conditions as discussed. The average rate of reduction in treated ground was 2.6% to 4.6% higher than untreated ground at the end of the repeated loading for 40% density ground. Similarly, a reduction rate of 1.5% to 3.5% higher was observed in 60% treated ground compared to untreated ground. For 40% relative density untreated ground, the initial void ratio of the soil was 0.77 before the start of tests, and the observed final void ratio was 0.70 at the end of 0.4g acceleration loading. With provision of reinforcement, the initial void ratio was observed to be 0.73 and final void ratio was 0.68. A similar pattern was also observed in 60% relative density, where the void ratio of the unreinforced deposit was reduced to 0.69 from 0.74 whereas in reinforced deposit, the void ratio reduced to 0.67 from 0.71. The faster reduction of void ratio in treated grounds during repeated loading may be due to the provision of drainage medium which induces faster dissipation of generated pore water pressure thereby inducing quicker soil deposition. Thus, the deposited soil bed forms a stable ground compared to untreated ground. Comparatively, 40% density treated ground showed maximum reduction in void ratio as compared to 60% density treated ground. This also evidenced that, combined drainage and reinforcement barrier performs well in loose sand conditions and can improve the seismic resistance of the ground deposit. From the estimated void ratio values and improvement in cone penetration values, it is clear that the provided reinforcement barrier performs better under repeated loading events.

5.6 Foundation Settlement

To evaluate the efficiency of confined barrier system, a scaled foundation model was placed at center of the prepared ground. The details of the footing selected for the study was already explained in Section 4.2. The

observed foundation settlements with respect to incremental sequential amplitude accelerations for both reinforced and unreinforced soil deposits prepared for 40% and 60% relative density is shown in Fig. 19. It can be seen that, provision of lateral confinement and drainage improves the seismic performance of saturated ground and minimizes foundation settlement during repeated acceleration loading conditions. As seen from acceleration response, the barrier system attenuates incoming motions to the structure placed within the confined zone. Also, the installed granular drains minimize generation of pore water pressures and improves dissipation rate thereby improving soil densification to enhance the stability of the model footing. As discussed, continuous generation of pore water pressure from bottom to top made soil at shallow depth more susceptible to liquefaction in untreated ground. This can be evident from the obtained foundation settlement at 40% and 60% untreated ground. Comparatively, ground having 40% density experienced more settlement than 60% ground. Further, the non-uniform density with depth contributes to additional reduction in the strength of deposit under repeated loading events. However, with the provision of drains and barrier confinement, the seismic response of the ground improved at low to medium acceleration loading events. In case of treated ground, no settlement was observed at 0.1g acceleration loading in case of 60% dense ground whereas very limited settlement was observed at 0.1g acceleration loading in case of 40% dense ground. The reduction of foundation settlement in treated ground ranges from 90% to 57% at 40% density condition and 98% to 56% at 60% density condition under incremental loading conditions. Occurrence of foundation settlement is mainly due to continuous generation of pore water pressure and column clogging observed during repetitive loading. It is also evident from both treated and untreated ground that, in addition to drainage; improvement in density also plays a major role in delaying pore pressure generation especially during repeated loading events. Thus, the PUF barrier system when incorporated with stone column reinforcement effectively mitigates the ground motion interaction with foundation and the effect of pore water pressure generation under repeated un-drained loading.

6 Conclusion

The primary intention of this research work is to develop and assess the performance of composite skirted ground reinforcement system in liquefaction mitigation and its associated ground deformations. Based on the obtained experimental test results, the following conclusions were made

- The proposed vibration barrier system is found effective in absorbing ground motions generated due to dynamic loading. The PUF isolation barrier confines foundation structure and improve its stability under repeated dynamic loading conditions. When this barrier system is incorporated with stone columns system, it is more effective and capable of mitigating both the generated ground motion interaction and the effect of pore water pressure generation during repeated loading.
- The continuous generation of pore water pressures from bottom to top and uneven soil deposition during repeated un-drained loading made soil at shallow depth more susceptible to liquefaction and reliquefaction. The developed composite skirted ground reinforcement system confines and increases the density of loose soil deposits which

improves the seismic resistance against re-liquefaction thereby improving the stability of foundation structure located at shallow depth.

- The time taken for attainment of peak value of pore water pressure decreases with the increase in acceleration. This suggesting that soil resistance against re-liquefaction reduces with the increase in intensity of the subsequent acceleration loading. With the provision of skirted ground reinforcement, it is observed that time taken for liquefaction increases under repeated loading due to combined drainage and densification effects offered together with ground motion attenuation which imparts stability to the structure even under repetitive loading conditions.

Acknowledgements

The authors would like to thank the Director, CSIR-Central Building Research Institute, Roorkee, for giving permission to publish this research work. The authors would also like to thank the Head, Geotechnical Engineering Division, CSIR-CBRI for his continuous support during this research work. Also, we would like to extend our thanks to the Head, Department of Applied Geophysics, IIT(ISM) Dhanbad and co-author, Dr. Saurabh Datta Gupta, Assistant Professor, Dept. of Applied Geophysics, IIT(ISM) Dhanbad, for their constant motivation and support during this research work.

Declarations

Funding - N.A
Conflict of Interest - N.A

References

1. Adam, M., & Von Estorff, O. (2005). Reduction of train-induced building vibrations by using open and filled trenches. *Computers & Structures*, *83*(1), 11-24. https://doi.org/10.1016/j.compstruc.2004.08.010
2. Ahmad, S., & Al-Hussaini, T. M. (1991). Simplified design for vibration screening by open and in-filled trenches. *Journal of geotechnical engineering*, *117*(1), 67-88.
3. Al-Hussaini, T. M., & Ahmad, S. (1991). Design of wave barriers for reduction of horizontal ground vibration. *Journal of geotechnical engineering*, *117*(4), 616-636.
4. Alzawi, A., & El Naggar, M. H. (2011). Full scale experimental study on vibration scattering using open and in-filled (GeoFoam) wave barriers. *Soil Dynamics and Earthquake Engineering*, *31*(3), 306-317.
5. Azzam, W., Ayeldeen, M., & El Siragy, M. (2018). Improving the structural stability during earthquakes using in-filled trench with EPS geofoam—numerical study. *Arabian Journal of Geosciences*, *11*(14), 1-11.
6. Baez, J. I., & Martin, G. R. (1993, May). Advances in the design of vibro systems for the improvement of liquefaction resistance. In *Symposium Ground Improvement* (pp. 1-16).
7. Banerjee, R., Konai, S., Sengupta, A., & Deb, K. (2017). Shake table tests and numerical modeling of liquefaction of Kasai River Sand. *Geotechnical and Geological Engineering*, *35*(4), 1327-1340.
8. Bhattacharya, S., Lombardi, D., Dihoru, L., Dietz, M. S., Crewe, A. J., & Taylor, C. A. (2012). Model container design for soil-structure interaction studies. *Role of seismic testing facilities in performance-based earthquake engineering*, 135-158.
9. Bose, T., Choudhury, D., Sprengel, J., & Ziegler, M. (2018). Efficiency of open and infill trenches in mitigating ground-borne vibrations. *Journal of Geotechnical and Geoenvironmental Engineering*, *144*(8), 04018048.
10. Bozorgnia, Y., & Campbell, K. W. (2004). The vertical-to-horizontal response spectral ratio and tentative procedures for developing simplified V/H and vertical design spectra. *Journal of Earthquake Engineering*, *8*(02), 175-207.
11. Bureau of Indian Standards (1976): *IS: 4968 (Part III) Method for Subsurface Sounding of Soils – Static Cone Penetration Test*. New Delhi, India: Bureau of Indian Standards.
12. Bureau of Indian Standards (1985): *IS: 2720 (Part IV) methods of test for soils – grain size analysis*. New Delhi, India: Bureau of Indian Standards.
13. Bureau of Indian Standards (2003): *IS: 15284 (Part1) Design and Construction for Ground Improvement - Guidelines*, C-2. New Delhi, India: Bureau of Indian Standards.
14. Connolly, D., Giannopoulos, A., Fan, W., Woodward, P. K., & Forde, M. C. (2013). Optimising low acoustic impedance back-fill material wave barrier dimensions to shield structures from ground borne high speed rail vibrations. *Construction and Building Materials*, *44*, 557-564.
15. Darby, K. M., Boulanger, R. W., et al (2019). Progressive changes in liquefaction and cone penetration resistance across multiple shaking events in centrifuge tests. *Journal of Geotechnical and Geoenvironmental Engineering*, *145*(3), 04018112.
16. Dasgupta, B. (1989). Vibration isolation of structures in a homogeneous elastic soil medium. Dissertation, *University of Minnesota, at Minneapolis*, in partial fulfillment of the requirements for the degree of Doctor of Philosophy.
17. Feng, S. J., Li, J. P., Zhang, X. L., Chen, Z. L., & Li, Y. C. (2020). Effects of water table on ground-borne vibration screening effectiveness by using open trenches. *Soil Dynamics and Earthquake Engineering*, *131*, 106031.
18. Hossain, M. Z., Abedin, M. Z., Rahman, M. R., Haque, M. N., & Jadid, R. (2021). Effectiveness of sand compaction piles in improving loose cohesionless soil. *Transportation Geotechnics*, *26*, 100451.
19. Hughes, J. M. O., Withers, N. J., & Greenwood, D. A. (1975). A field trial of the reinforcing effect of a stone column in soil. *Geotechnique*, *25*(1), 31-44.

20. Jamiolkowski, M., Lo Presti, D. C. F., & Manassero, M. (2003). Evaluation of relative density and shear strength of sands from CPT and DMT. In *Soil behavior and soft ground construction* (pp. 201-238). https://doi.org/10.1061/40659(2003)7
21. Kobayashi, T., Sassa, S., Watanabe, K., & Yamazaki, H. (2016). Shaking table tests of liquefaction in sand-clay layered ground and the effects of the ground compaction methods. In *Proc 7th Civil Engineering Conference in the Asian Region*.
22. Kunnath, S. K., Erduran, E., Chai, Y. H., & Yashinsky, M. (2008). Effect of near-fault vertical ground motions on seismic response of highway overcrossings. *Journal of Bridge Engineering*, *13*(3), 282-290. https://doi.org/10.1061/(ASCE)1084-0702(2008)13:3(282)
23. Lat, D. C., Ali, N., Jais, I. B. M., Yunus, N. Z. M., Razali, R., & Talip, A. R. A. (2020). A review of polyurethane as a ground improvement method. *Malaysian Journal of Fundamental and Applied Sciences*, *16*(1), 70-74.
24. Lee, C. J., Wei, Y. C., & Kuo, Y. C. (2012). Boundary effects of a laminar container in centrifuge shaking table tests. *Soil Dynamics and Earthquake Engineering*, *34*(1), 37-51.
25. Lombardi, D., & Bhattacharya, S. (2012). Shaking table tests on rigid soil container with absorbing boundaries. In *Proceedings of 15th World Conference on Earthquake Engineering, Lisbon, Portugal*.
26. Lombardi, D., Bhattacharya, S., Scarpa, F., & Bianchi, M. (2015). Dynamic response of a geotechnical rigid model container with absorbing boundaries. *Soil Dynamics and Earthquake Engineering*, *69*, 46-56.
27. Majumder, M., & Ghosh, P. (2016). Intermittent geofoam in-filled trench for vibration screening considering soil non-linearity. *KSCE Journal of Civil Engineering*, *20*(6), 2308-2318. https://doi.org/10.1007/s12205-015-0267-6
28. Moncarz, P. D., & Krawinkler, H. (1981). *Theory and application of experimental model analysis in earthquake engineering* (Vol. 50). California: Stanford University.
29. Muley, P., Maheshwari, B. K., & Paul, D. K. (2015). Liquefaction potential of Roorkee region using field and laboratory tests. *International Journal of Geosynthetics and Ground Engineering*, *1*(4), 1-13.
30. Murali Krishna, A., & Madhavi Latha, G. (2007). Seismic response of wrap-faced reinforced soil-retaining wall models using shaking table tests. *Geosynthetics International*, *14*(6), 355-364.
31. National Co-operative Highway Research Program (NCHRP) Synthesis 368, Cone penetration testing guidelines, pg.-41
32. Padmanabhan, G., & Shanmugam, G. K. (2020). Reliquefaction Assessment Studies on Saturated Sand Deposits under Repeated Acceleration Loading Using 1-g Shaking Table Experiments. *Journal of Earthquake Engineering*, 1-23. https://doi.org/10.1080/13632469.2020.1778588
33. Papazoglou, A. J., & Elnashai, A. S. (1996). Analytical and field evidence of the damaging effect of vertical earthquake ground motion. *Earthquake Engineering & Structural Dynamics*, *25*(10), 1109-1137.
34. Pu, X., Shi, Z., & Xiang, H. (2018). Feasibility of ambient vibration screening by periodic geofoam-filled trenches. *Soil Dynamics and Earthquake Engineering*, *104*, 228-235.
35. Punetha, P (2016) Study on seismic isolation of buildings using geosynthetics. M.Tech Dissertation, *AcSIR, CSIR – Central Building Research Institute*, Roorkee.
36. Robertson, P. K., & Campanella, R. G. (1985). Liquefaction potential of sands using the CPT. *Journal of geotechnical engineering*, *111*(3), 384-403.
37. Seed, H. B., & Lee, K. L. (1966). Liquefaction of saturated sands during cyclic loading. *Journal of the Soil Mechanics and Foundations Division*, *92*(6), 105-134.
38. Singh, H. P. (2009). *Liquefaction studies of composite materials* (Doctoral dissertation, Ph. D. thesis, Dept. of Earthquake Engineering, Indian Institute of Technology, Roorkee, India).
39. Tsuchida, H. (1970). Evaluation of liquefaction potential of sandy deposits and measures against liquefaction induced damage. In *Proceedings of the annual seminar of the Port and Harbour Research Institute* (pp. 3-1).
40. Vaid, Y. P., & Negussey, D. (1988). Preparation of reconstituted sand specimens. In *Advanced triaxial testing of soil and rock*. ASTM International.

41. Varghese, R. M., & Latha, G. M. (2014). Shaking table tests to investigate the influence of various factors on the liquefaction resistance of sands. *Natural hazards*, *73*(3), 1337-1351.
42. Wang, J. G., Sun, W., & Anand, S. (2009). Numerical investigation on active isolation of ground shock by soft porous layers. *Journal of sound and vibration*, *321*(3-5), 492-509.
43. Wang, S., Yang, J., & Onyejekwe, S. (2013). Effect of previous cyclic shearing on liquefaction resistance of Mississippi River Valley silt. *Journal of materials in civil engineering*, *25*(10), 1415-1423. https://doi.org/10.1061/(ASCE)MT.1943-5533.0000698
44. Wang, Z. L., Li, Y. C., & Wang, J. G. (2006). Numerical analysis of attenuation effect of EPS geofoam on stress-waves in civil defense engineering. *Geotextiles and Geomembranes*, *24*(5), 265-273.
45. Whitman, R. V., & Lambe, P. C. (1986). Effect of boundary conditions upon centrifuge experiments using ground motion simulation. *Geotechnical Testing Journal*, *9*(2), 61-71. https://doi.org/10.1520/GTJ11031J
46. Woods, R. D. (1968). Screening of surface waves in soils, The *University of Michigan* Industry Program of the College of Engineering. *IP-804*.
47. Xenaki, V. C., & Athanasopoulos, G. A. (2003). Liquefaction resistance of sand–silt mixtures: an experimental investigation of the effect of fines. *Soil Dynamics and Earthquake Engineering*, *23*(3), 1-12.
48. Yang, W., Yuan, R., & Wang, J. (2018). Vibration induced by subway trains: open-trench mitigation analysis in the time and frequency domains. *Shock and Vibration*, *2018*.
49. Yang, Y. B., & Hung, H. H. (1997). A parametric study of wave barriers for reduction of train-induced vibrations. *International journal for numerical methods in engineering*, *40*(20), 3729-3747.
50. Ye, B., Hu, H., Bao, X., & Lu, P. (2018). Reliquefaction behavior of sand and its mesoscopic mechanism. *Soil Dynamics and Earthquake Engineering*, *114*, 12-21. https://doi.org/10.1016/j.soildyn.2018.06.024
51. Youd, T. L. (1984). Recurrence of liquefaction at the same site. In *Proc. 8th World Conf. Earthq. Engng* (Vol. 3, pp. 231-238). Prentice-Hall Inc.
52. Zeng, X., Rose, J. G., & Rice, J. S. (2001). Stiffness and damping ratio of rubber-modified asphalt mixes: Potential vibration attenuation for high-speed railway trackbeds. *Journal of Vibration and Control*, *7*(4), 527-538. https://doi.org/10.1177%2F107754630100700403

List of Figures

List of Tables

Figures

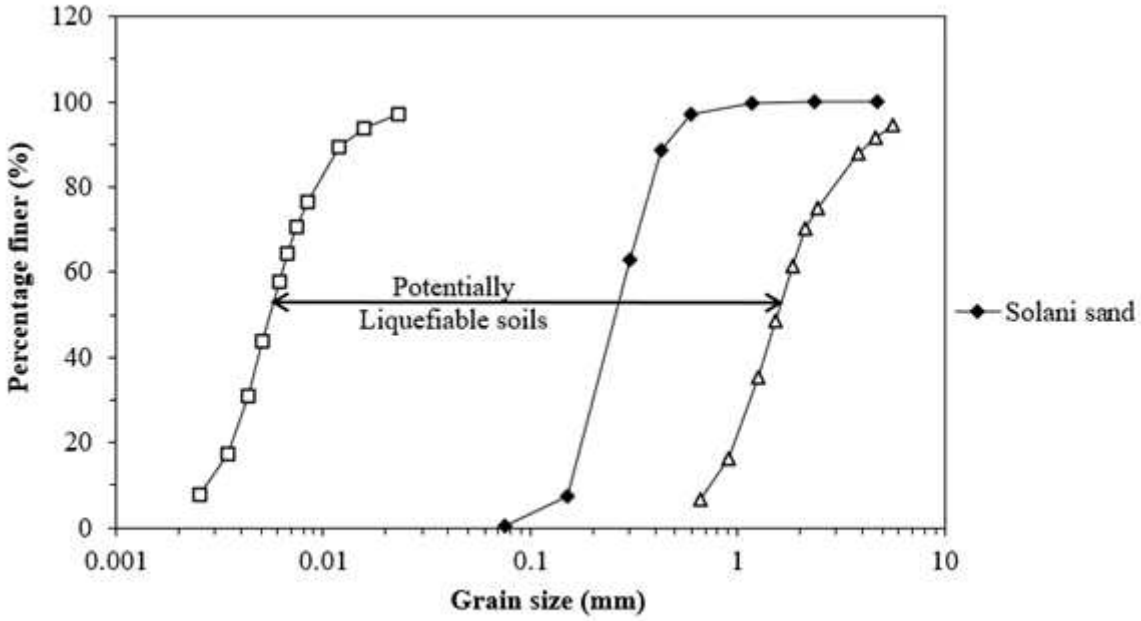

Figure 1

Comparison of Grain size distribution curve of solani sand with potentially liquefiable soils.

(a)

(b)

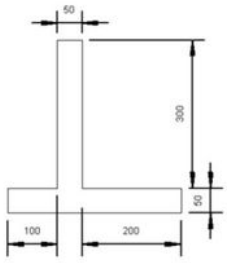

Figure 2

PU Foam barrier preparation (a) Moulds wrapped with geotextile for PUF barrier casting; (b) PU-foam barrier casting and preparation carried out in standard shear boxes; (c) Finished top, side and sectional views of prepared PU Foam barriers

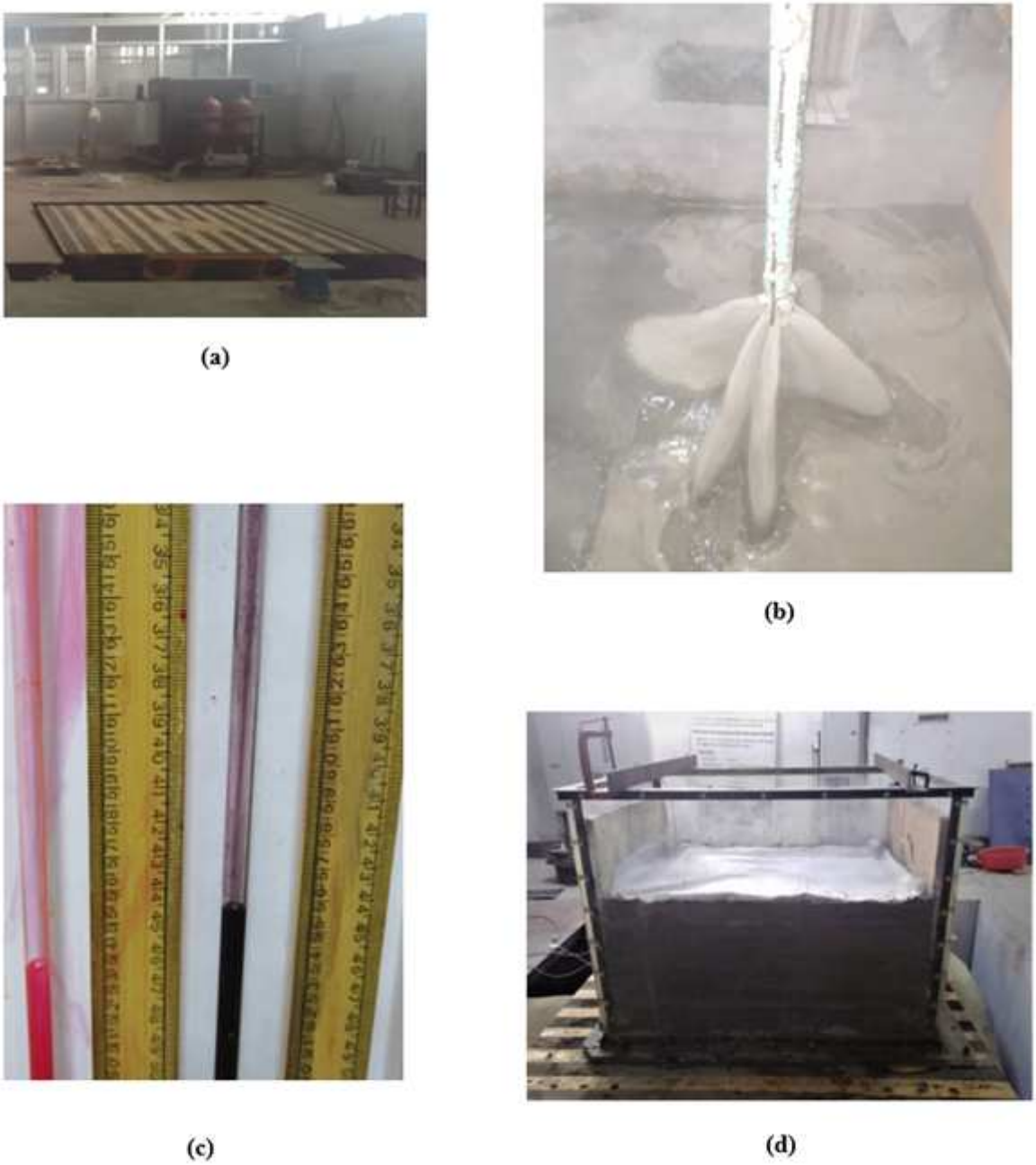

Figure 3

Shaking table test setup and method of sample preparation (a) Uni-axial shaking table facility with servo-controlled pump system at CSIR-CBRI; (b) Preparation of the model ground by Wet pluviation technique; (c) Glass piezometers with red and black coloured liquids connected to the prepared sand bed at 0.4m and 0.2m depth from prepared ground bed surface respectively; (d) Side view of the prepared model ground covered with geotextile before the commencement of experiments

(a)

(b)

(c)

Figure 4

Installation of stone columns (a) Extraction of soil inside casing area using auger; (b) First layer of stone filling carried out inside the casing area; (c) Compaction of the layer by tamping and lifting to proceed with next layer

(a)

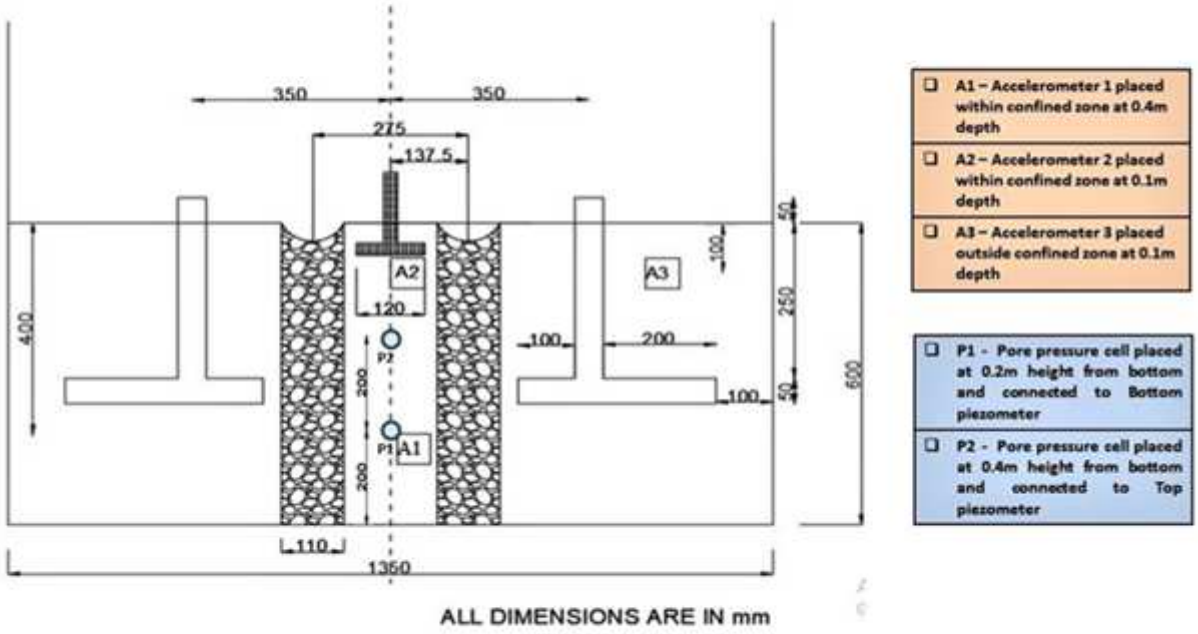

(b)

Figure 5

Model ground with skirted ground reinforcement system and their accelerometer and piezometer connection details (a) Top view ; (b) Sectional view

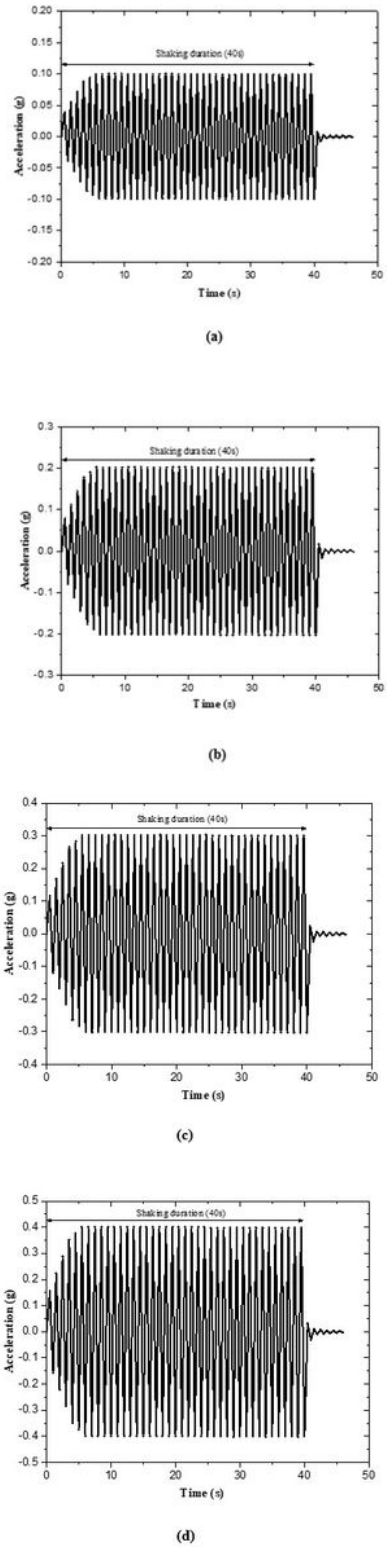

Figure 6

Time history for selected input motions (a) 0.1g; (b) 0.2g; (c) 0.3g; (d) 0.4g

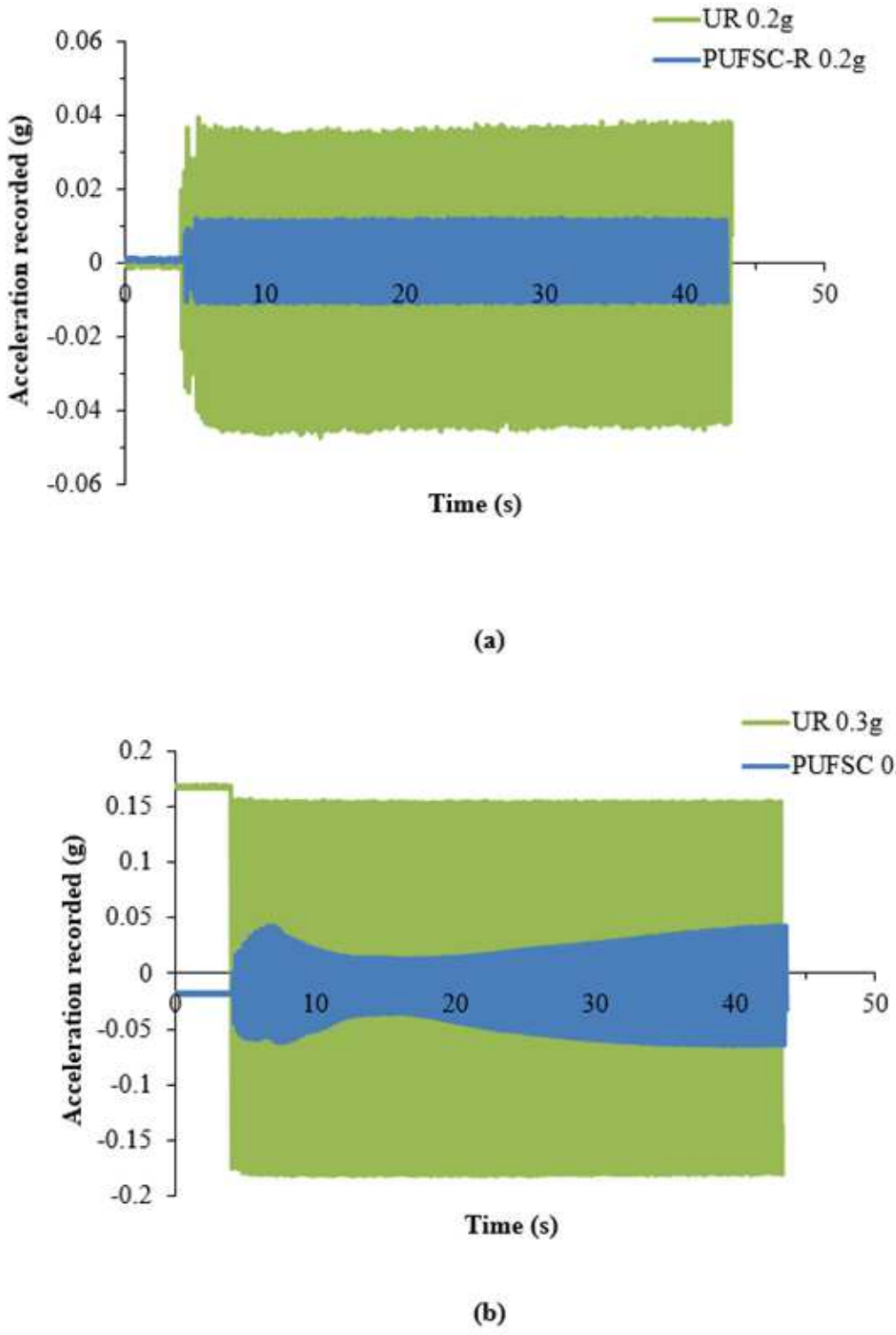

Figure 7

Typical acceleration response of Un-Reinforced model ground [UR] and PU Foam Skirted ground Reinforced model ground [PUFSC-R] at (a) 40% density at 0.2g acceleration loading; (b) 60% density at 0.3g acceleration loading

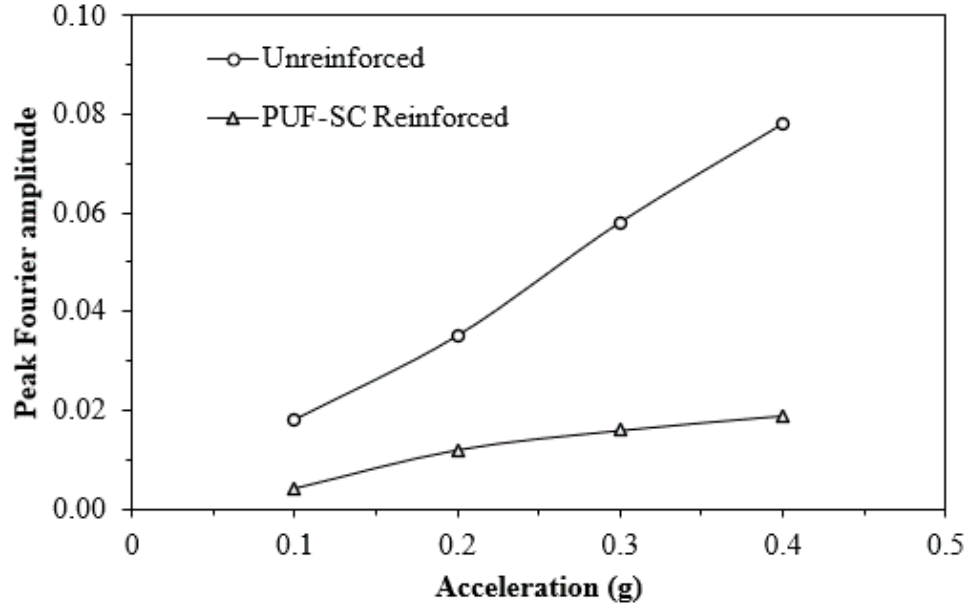

(a)

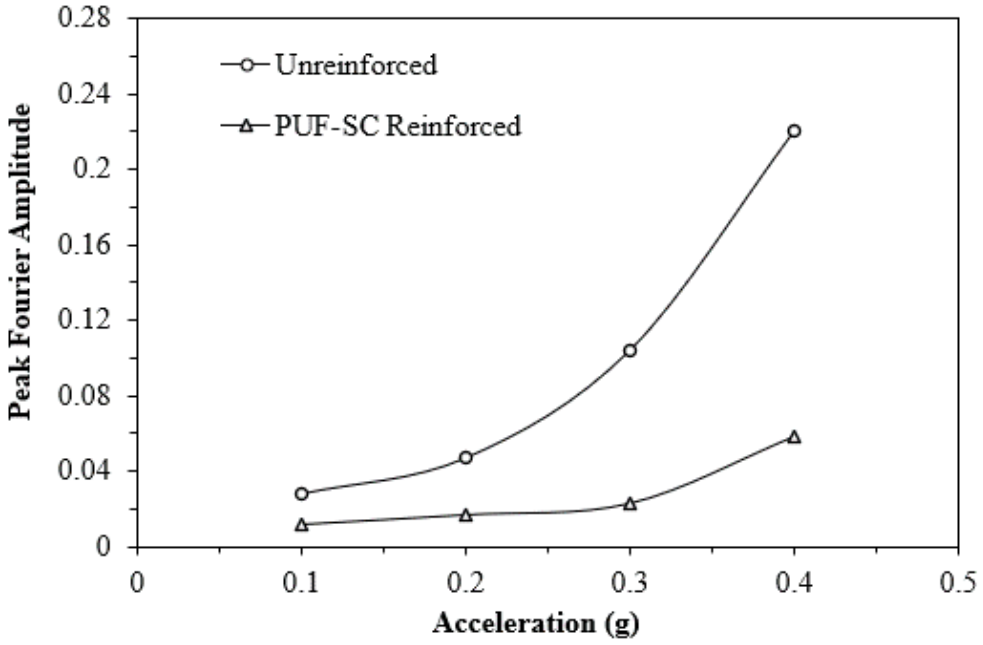

(b)

Figure 8

Comparison of peak Fourier amplitude near foundation model with skirted ground reinforcement [PUF-SC] system and unreinforced system under sub-sequential loading in the prepared (a) 40% density ground (b) 60% density ground

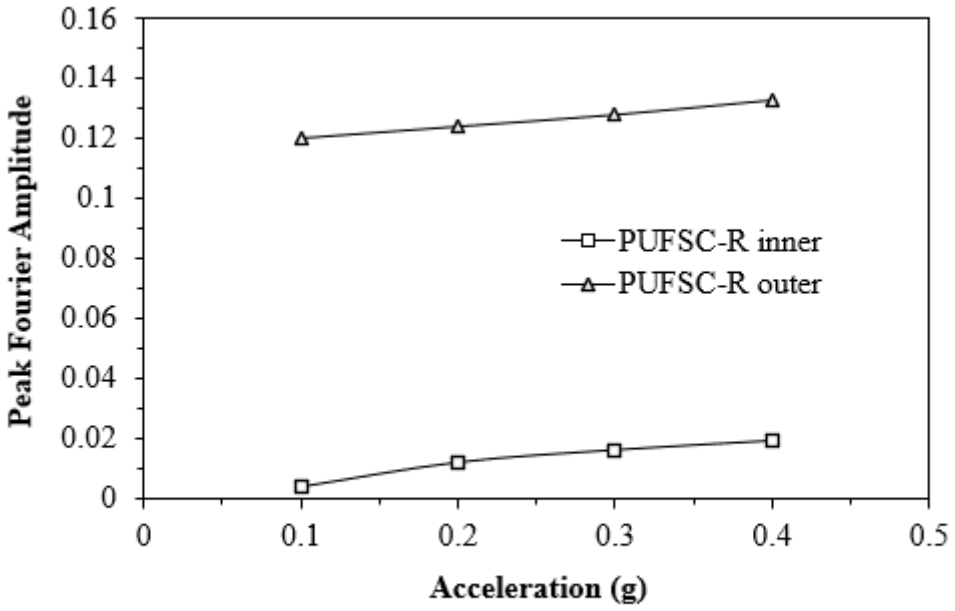

(a)

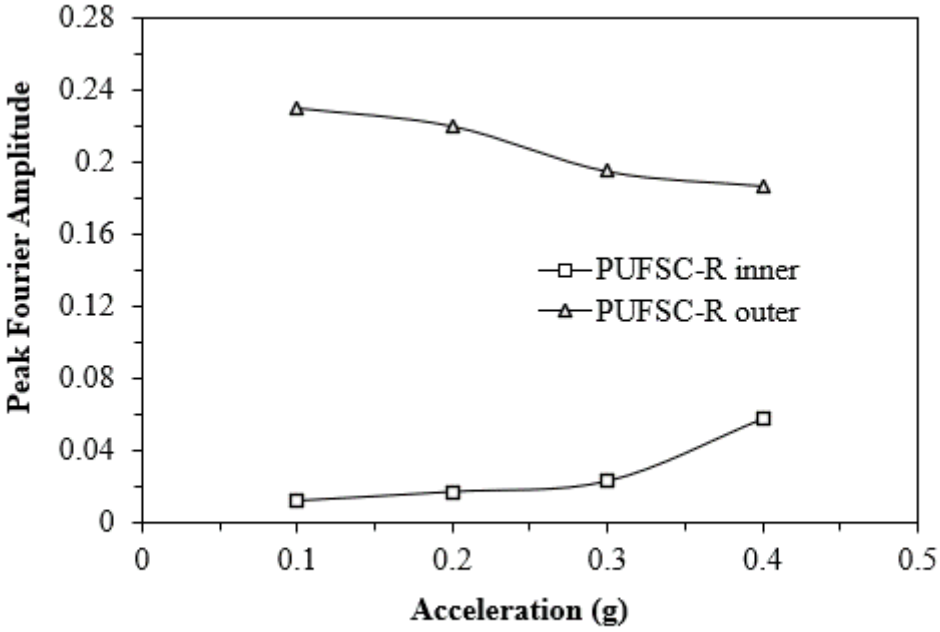

(b)

Figure 9

Acceleration response obtained from accelerometer placed outside and inside the confined zone of skirted ground reinforcement [PUFSC-R] system (a) 40% ground (b) 60% ground

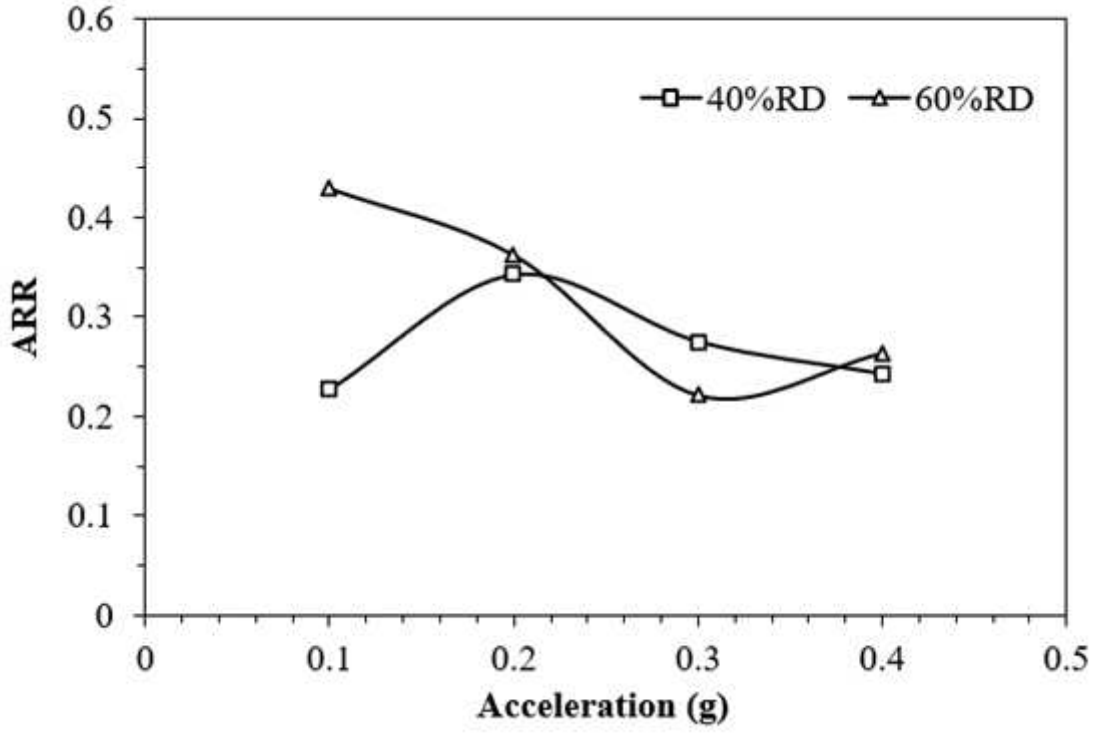

Figure 10

Comparative amplitude reduction ratio (ARR) for the selected skirted ground reinforcement system under sequential loading conditions

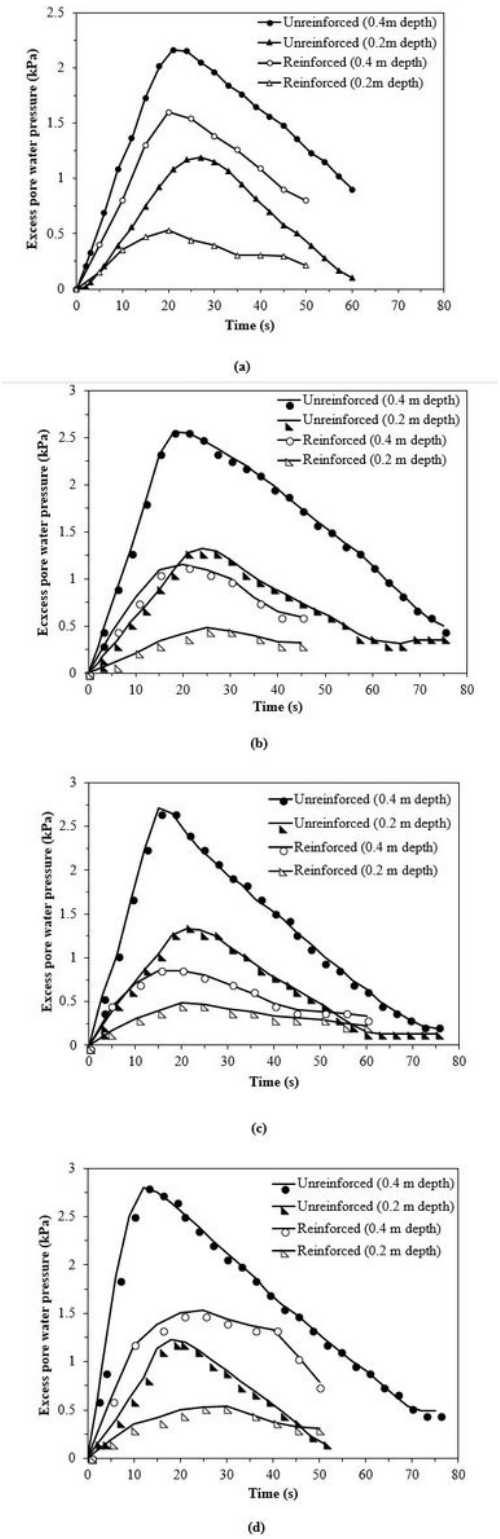

Figure 11

Excess pore water pressure generation with time recorded by piezometers placed at 0.4m and 0.2m depth from the prepared ground bed surface in unreinforced and reinforced ground at 40% density (a) 0.1g (b) 0.2g (c) 0.3g (d) 0.4g

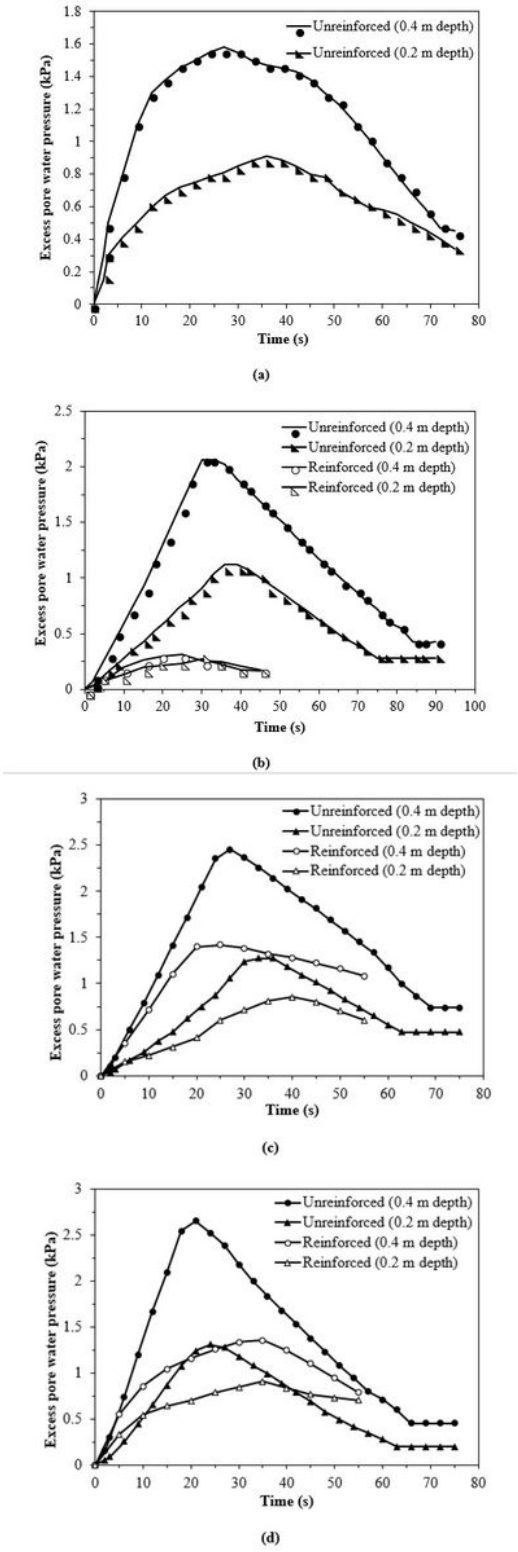

Figure 12

Excess pore water pressure generation with time recorded by piezometers placed at 0.4m and 0.2m depth from the prepared ground bed surface in the unreinforced and reinforced ground at 60% density (a) 0.1g (b) 0.2g (c) 0.3g (d) 0.4g

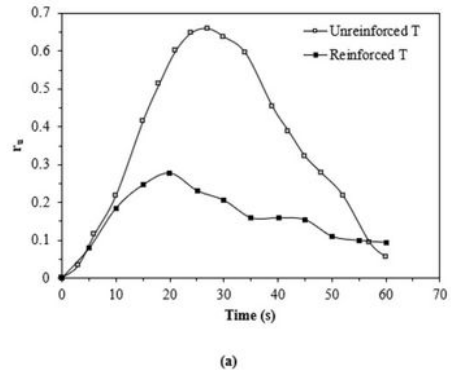

(a)

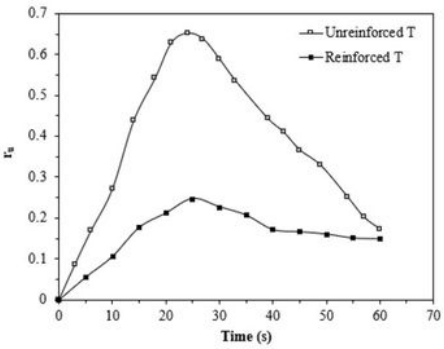

(b)

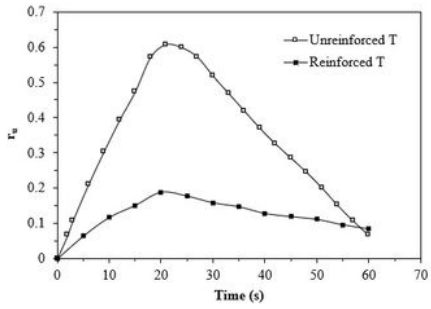

(c)

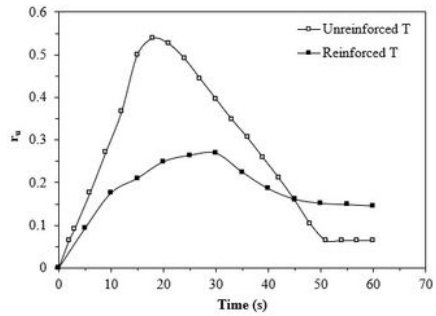

(d)

Figure 13

Pore pressure ratio [ru] with time for the unreinforced and reinforced ground prepared for 40% density at Top [T] 0.2m depth (a) 0.1g (b) 0.2g (c) 0.3g (d) 0.4g

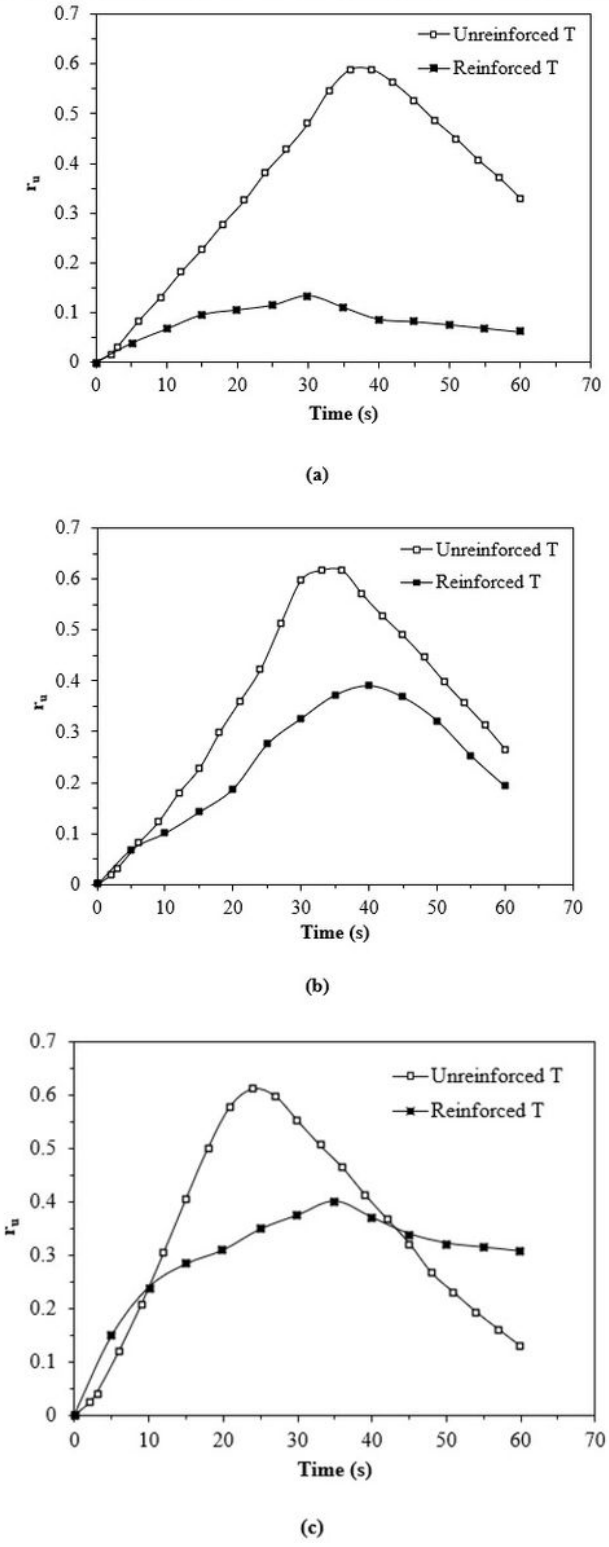

Figure 14

Pore pressure ratio [ru] with time for the unreinforced and reinforced ground prepared for 60% density at Top [T] 0.2m depth (a) 0.2g (b) 0.3g (c) 0.4g

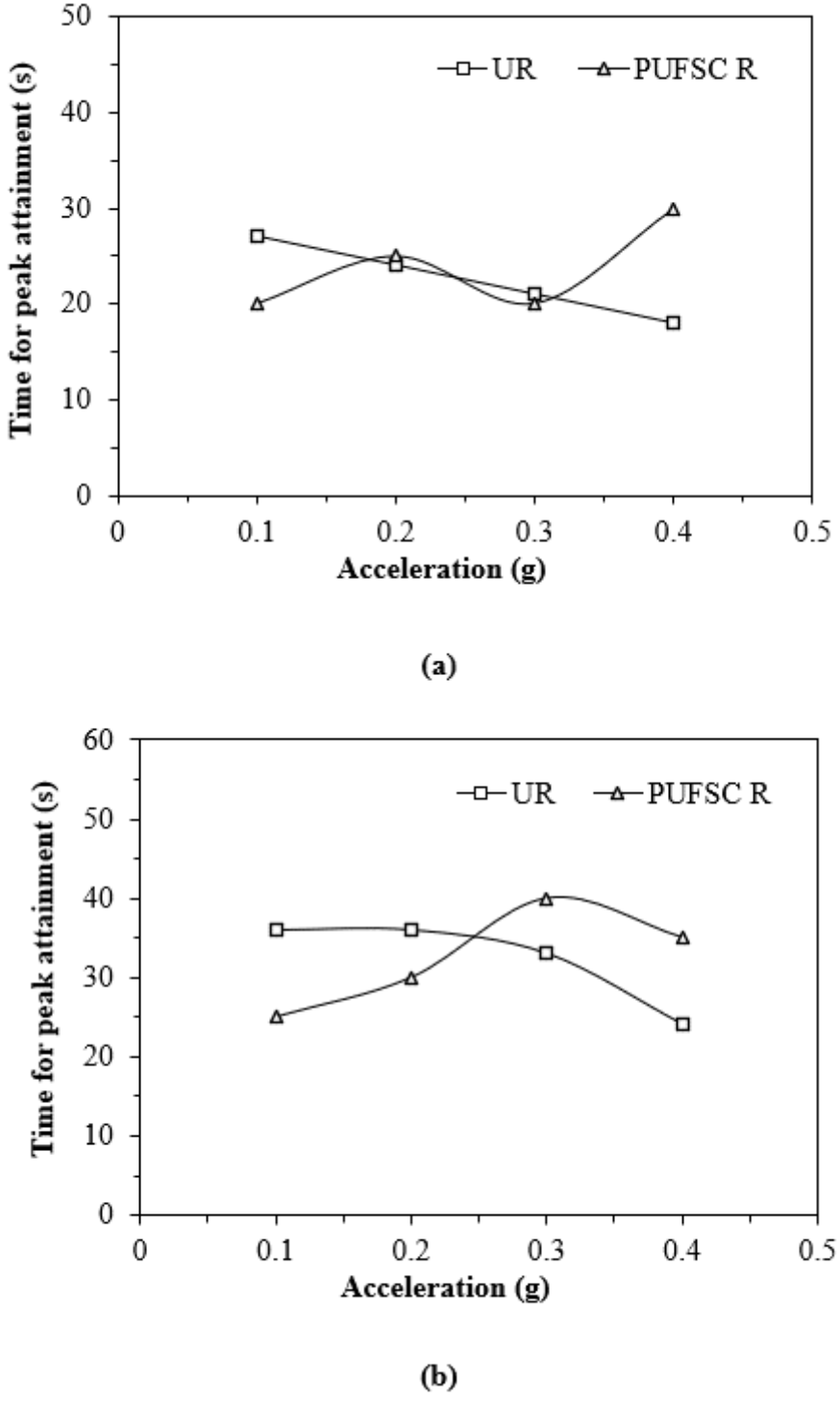

Figure 15

Time taken for attainment of peak value of pore pressure in unreinforced [UR] and skirted ground reinforced [PUFSC-R] soil deposits under repeated loading conditions when prepared for (a) 40% density condition (b) 60% density condition.

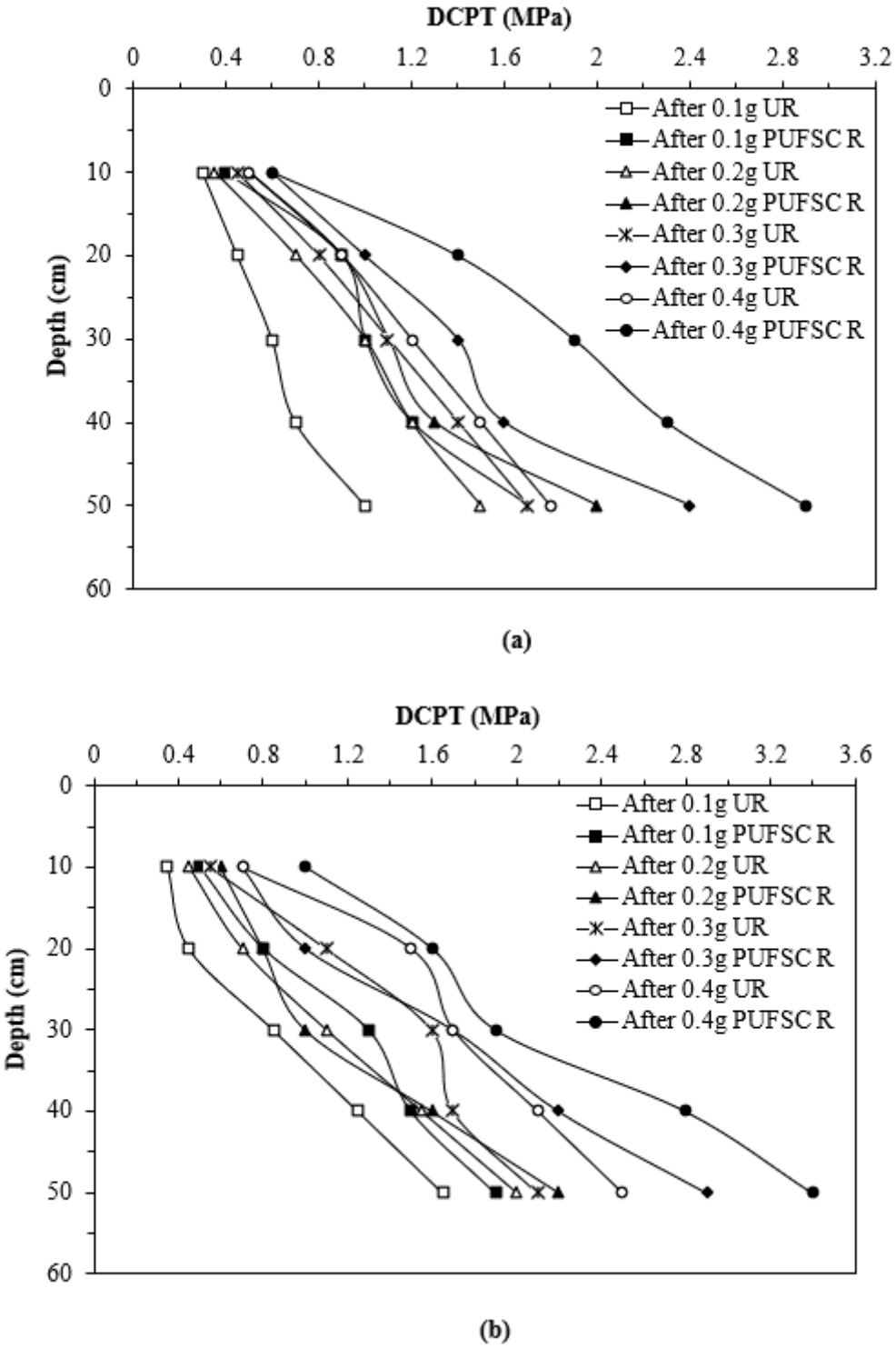

Figure 16

Cone penetration resistance values for the unreinforced [UR] and skirted ground reinforced [PUFSC-R] soil deposits under repeated loading conditions when prepared for (a) 40% density condition (b) 60% density condition.

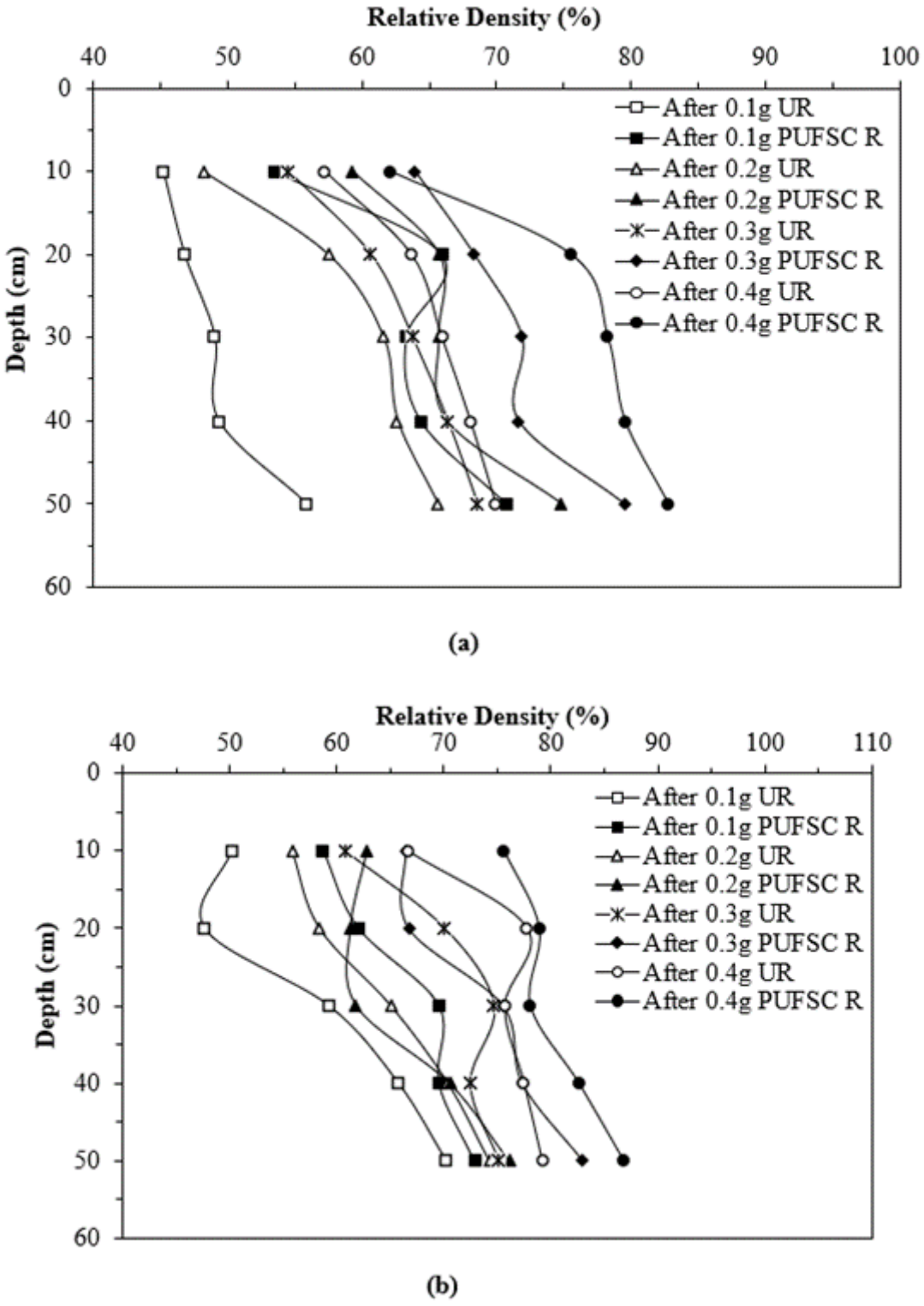

Figure 17

Relative Density variation for the unreinforced [UR] and skirted ground reinforced [PUFSC-R] soil deposits under repeated loading conditions when prepared for (a) 40% density condition (b) 60% density condition.

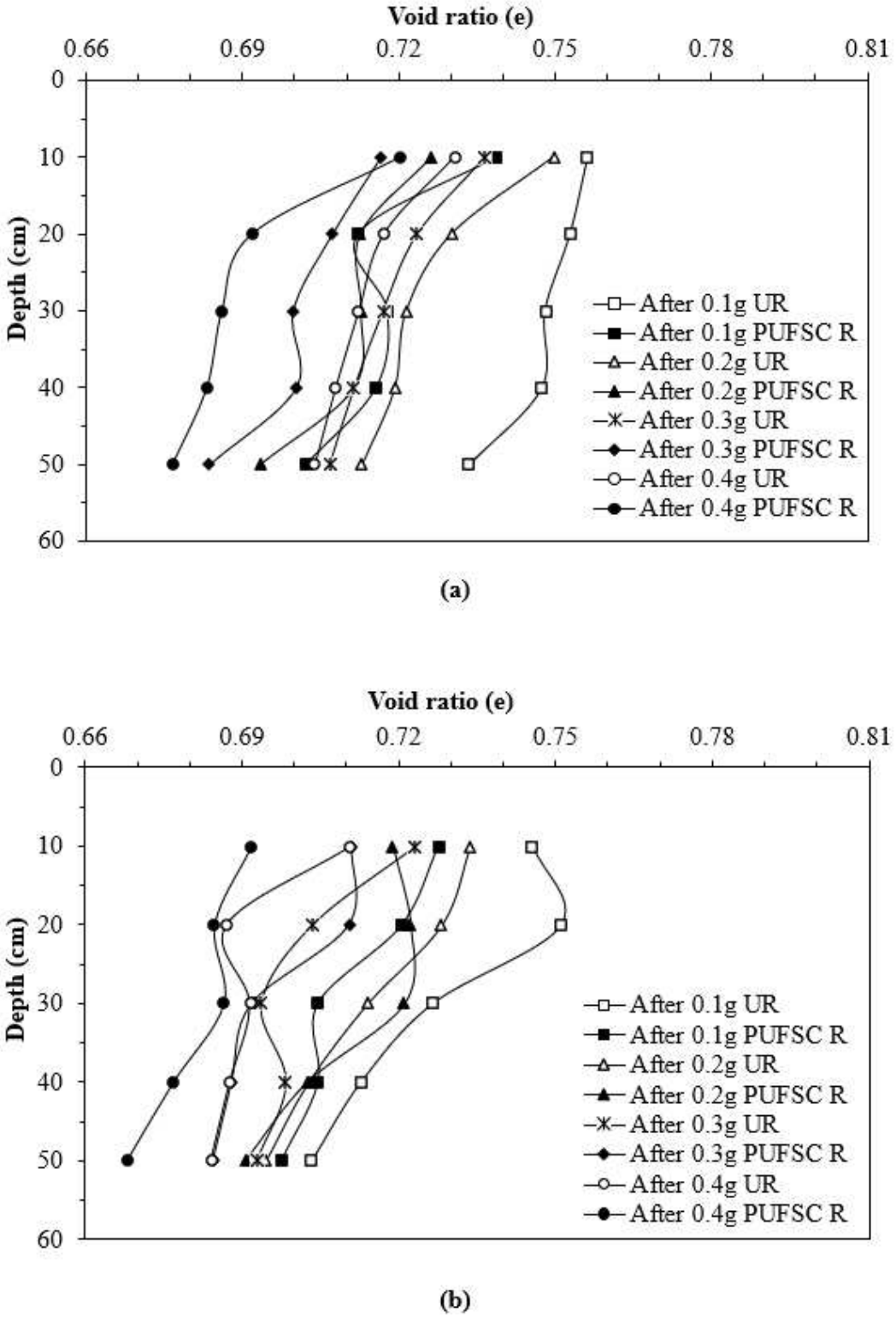

Figure 18

Void ratio variations with respect to depth for unreinforced [UR] and skirted ground reinforced [PUFSC-R] soil deposit under repeated loading conditions when prepared for (a) 40% density condition (b) 60% density condition.

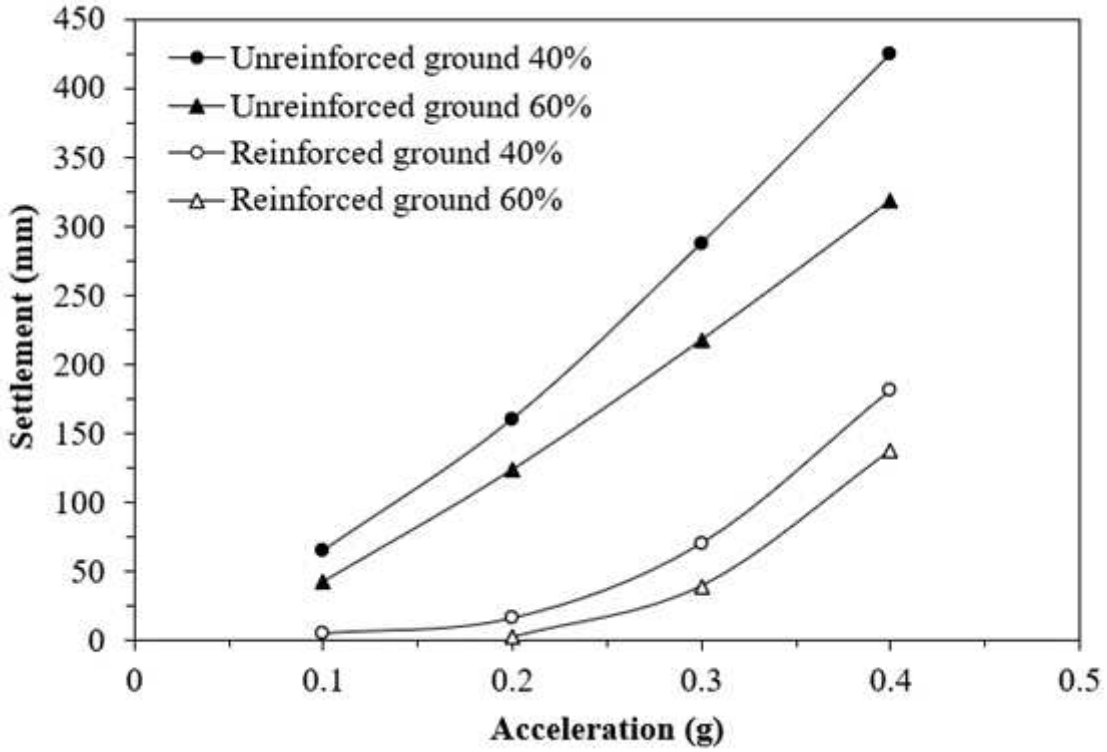

Figure 19

Observed cumulative foundation settlement with acceleration loading for unreinforced and reinforced ground conditions.

Supplementary Files

This is a list of supplementary files associated with this preprint. Click to download.

- Supplementaryfigures.docx
- TableRevised.docx